Research Square

Preprints are preliminary reports that have not undergone peer review.
They should not be considered conclusive, used to inform clinical practice,
or referenced by the media as validated information.

Stabilizing Quantum Effects in Open Systems Through Dynamic Coupling Modulation

Amir Rahmani
Alireza Dehghani
alireza.dehghani@gmail.com

Sahand University of Technology
Parisa Rezaei
K Jamshidi-Ghaleh

Research Article

Keywords: Quantum Frequency Conversion, Time-Dependent Coupling, Quantum Entanglement, Photon Blockade, Non-classical Light, Quantum Control, Open Quan- tum Systems

Posted Date: September 10th, 2026

DOI: https://doi.org/10.21203/rs.3.rs-9885248/v1

License: This work is licensed under a Creative Commons Attribution 4.0 International License.
Read Full License

Additional Declarations: No competing interests reported.

Stabilizing Quantum Effects in Open Systems Through Dynamic Coupling Modulation

A. Rahmani[1*], A. Dehghani[2,3†], P. Rezaei[4‡] and K. Jamshidi-Ghaleh[4§]

[1] *Institute of Physics Polish Academy of Sciences, Al. Lotników 32/46, 02-668 Warsaw, Poland*

[3] *Department of Physics, Sahand University of Technology, Tabriz, Iran*

[2] *Department of Physics, Payame Noor University, Tehran, Iran*

[4] *Department of Physics, Azarbaijan University of Tarbiat Moallem, Tabriz, Iran*

June 4, 2026

Abstract

This work transforms the quantum frequency converter (QFC) from a passive transducer into an actively controllable quantum interface through dynamic control of its coupling coefficient $\kappa(t)$. While conventional parametric amplifiers are inherently noisy, the QFC represents a fundamental, noiseless limit of quantum parametric interaction. By engineering $\kappa(t)$ to be time-dependent, we demonstrate that a single modulation waveform achieves what previously required multiple nonlinear components: entanglement generation from initially separable states, suppression of entanglement sudden death, strong photon antibunching, and—remarkably—two-photon blockade without intrinsic nonlinearity, induced purely through temporal control. This work does not merely optimize an existing device—it redefines its function. By showing that a single, experimentally simple modulation can induce nonlinear quantum phenomena in a linear system, stabilize entanglement against decoherence, and provide exact analytical control, we establish dynamic coupling modulation as a new paradigm for quantum state engineering in any bilinear, parametrically driven platform.

Keywords: Quantum Frequency Conversion, Time-Dependent Coupling, Quantum Entanglement, Photon Blockade, Non-classical Light, Quantum Control, Open Quantum Systems.

1 Introduction

The advent of high-power laser sources has been a cornerstone in the advancement of quantum optics, nonlinear optics, and laser spectroscopy. When a high-powered laser interacts

*Email:rahmani@ifpan.edu.pl

†Corresponding Author, Email: alireza.dehghani@gmail.com, adehghani@pnu.ac.ir

‡Email: prezaee150@gmail.com

§Email: k-jamshidi@azaruniv.ac.ir

with a nonlinear crystal, it can generate and amplify a spectrum of new optical frequencies, a process fundamental to creating non-classical states of light such as squeezed states [1, 2]. In recent decades, significant research efforts have been directed toward understanding and harnessing the non-classical properties of electromagnetic fields [3], driven by their pivotal applications in quantum computing [4], quantum communication [4], and quantum cryptography [5]. Notable examples include the use of squeezed states for secure cryptographic protocols [5], the long-distance transmission of coherent states for quantum teleportation [6], the exploitation of photon anti-bunching to create on-demand single-photon sources [7], and the utilization of entanglement for continuous-variable quantum information processing [8, 9].

In this work, we challenge and fundamentally reframe this perspective. We demonstrate that by introducing dynamic, time-dependent control of the intercavity coupling coefficient $\kappa(t)$, the quantum frequency converter (QFC) is transformed from a passive transducer into an active, controllable quantum interface. This paradigm shiftfrom static [10] to dynamic parametric interactionunlocks capabilities previously thought to require separate, often incompatible, nonlinear components. This perspective is further supported by very recent work from Falch et al. [11], who independently demonstrate that in ultrastrongly coupled cavity-magnon systems, non-classical features such as antibunching can arise purely from the counter-rotating terms of a linear interaction Hamiltonian. Their findings reinforce the growing understanding that engineered linear interactions, under the right conditions, can be a powerful resource for quantum state engineering. Specifically, we show that a single, experimentally simple modulation waveform can simultaneously induce nonlinear quantum effects in a nominally linear system, stabilize entanglement against sudden death, and generate multi-photon non-classical states, all within a unified and analytically solvable framework.

A quintessential process in this domain is the nonlinear response of a medium to an intense pump field, which facilitates controlled energy exchange between electromagnetic fields of different frequencies [12]. Among these nonlinear interactions, parametric amplification and quantum frequency conversion (QFC) are of paramount importance. The foundational quantum mechanical model for these parametric interactions, established by Louisell, Yariv, and Siegman [12], treats the coupling coefficient κ as a constant. In a quantum parametric amplifier (QPA), a pump photon of frequency ω_p is annihilated to create a correlated signal-idler photon pair ($\omega_p = \omega_a + \omega_b$), generating highly entangled two-mode squeezed vacuum states. However, this process is inherently probabilistic and represents a fundamental source of quantum noise in amplifiers. In contrast, the quantum frequency converter operates under the condition $\omega_p = \omega_a - \omega_b$, enabling a deterministic, coherent transfer of a photon from one frequency to another ($|n_a, n_b\rangle \rightarrow |n_a + 1, n_b - 1\rangle$) [12]. This distinct mechanism makes the QFC a potentially noiseless transducer, indispensable for interfacing disparate quantum systems in a quantum network [13, 14].

In section 2 of this work, we begin by analyzing conventional quantum parametric interactions and discussing their inherent limitations. As detailed in subsection 2.1, while parametric processes can generate entanglement, they suffer from fundamental constraints including the inherent instability of quantum correlations, susceptibility to environmental decoherence, and the transient nature of generated entanglement states. These limitations become particularly apparent in open quantum systems where entanglement sudden death and revival phenomena pose significant challenges for practical quantum technologies. The

static nature of traditional coupling coefficients in these systems restricts our ability to actively control and stabilize quantum correlations against these detrimental effects.

This research gap motivates the paradigm shift we explore in the present work: transitioning from static parametric systems to dynamically controlled quantum frequency converters with explicitly time-dependent coupling coefficients $\kappa(t)$. While previous studies have analyzed QFCs with time-dependent pump amplitudes [15] or within static, lossy frameworks [16, 17], a comprehensive treatment of a QFC with a dynamically modulated inter-cavity coupling remains an open frontier. We advance the theoretical framework by introducing a model where $\kappa(t)$ serves as an active control parameter. The high-power classical pump field provides the energy source that activates the nonlinear interaction, while the initial quantum states of the cavities constitute the programmable input whose quantum propertiessuch as photon statistics and entanglementare dynamically shaped by this engineered coupling. In our model, a high-power classical pump field drives the nonlinear crystal, providing the energy necessary for frequency conversion, while the signal and idler modes are initialized in weak quantum states (e.g., single-photon or few-photon Fock states). This configuration is standard in quantum nonlinear optics, where strong pumps enable deterministic manipulation of non-classical light without themselves introducing quantum noise into the signal modes.

To navigate the complexities of this time-dependent Hamiltonian, where standard methods like the Dyson series or the Lewis-Riesenfeld invariant approach [18, 19, 20] can be computationally prohibitive or approximate, we derive an **exact, closed-form** analytical time-evolution operator for the system. This operator provides a versatile and powerful tool for analyzing the system's dynamics from arbitrary initial states, revealing that the entire dynamics are governed by a single complex function $d(t)$ satisfying a Riccati-type equationa structural revelation that transcends conventional approximate methods.

To preempt any ambiguity regarding the novelty and scope of this work, we explicitly enumerate the four distinct contributions that, in aggregate, constitute a qualitative leap beyond the state of the art:

♠ **From Static to Dynamic Quantum Frequency Conversion:** Prior work on quantum frequency conversion (QFC)-from the foundational Louisell-Yariv-Siegman model [12] to recent implementations in quantum networks [13, 14]-treats the coupling coefficient κ as either constant or adiabatically varying. We demonstrate that temporal modulation of $\kappa(t)$ transforms the QFC from a passive device into an active, controllable quantum interface. It serves as a universal entangler, generating quantum correlations from any initial separable state while providing a potent mechanism to combat the inherent "entanglement sudden death" observed in static parametric interactions-a capability we explicitly quantify and visualize in Section 4.

♠**Exact Analytical Solution for a Time-Dependent, Non-Stationary Hamiltonian:** Time-dependent quadratic Hamiltonians are typically approached via the Lewis-Riesenfeld invariant or Dyson series approximations. We derive an exact, closed-form time-evolution operator for the dynamically modulated QFC. This is not merely a computational convenience-it is a structural revelation: the entire dynamics are governed by a single complex function $d(t)$ satisfying a Riccati-type equation. This analytical tractability is extremely rare in non-stationary quantum optics and provides a universal template for any bilinear, parametrically driven system (optical, microwave, mechanical).

♠**Two-Photon Blockade Without Intrinsic Nonlinearity:** Conventional photon blockade requires strong $\chi^{(3)}$ nonlinearities -$g^{(2)}(t) \geq 1$ coexisting with $g^{(3)}(t) \ll 1$-is achieved with the simple modulation $\kappa(t) = \frac{1}{2}\cos^2(t/2)$. This is not a perturbative effect; it is a dynamical nonlinearity induced purely by temporal control. This extends the phenomenon of photon blockade into regimes previously considered inaccessible.

♠**Unified Control of Entanglement, Photon Statistics, and Decoherence Resistance:** In conventional architectures, entanglement generation, photon shaping, and decoherence mitigation require separate, often incompatible, components. Our framework shows that a single time-dependent parameter $\kappa(t)$ simultaneously: (i) generates entanglement from any separable input state; (ii) suppresses entanglement sudden death; (iii) produces strong antibunching and two-photon blockade; and (iv) confers measurable robustness against Markovian dissipation. Our analysis, conducted via the Lindblad master equation, reveals that while dissipation naturally degrades quantum correlations, the benefits of dynamic control persist, offering a pathway to protect quantum resources in open systems.

This paper is structured as follows: In section 2, we analyze conventional quantum parametric interactions and their limitations, with subsection 2.1 specifically examining entanglement generation in these systems. Section 3 revisits the quantum frequency conversion framework as a solution to these limitations. Section 4 presents our core contribution: optimal entanglement generation in time-dependent quantum frequency converters via dynamical control of the inter-cavity coupling coefficient. The engineering of photon anti-bunching and the two-photon blockade process is thoroughly investigated in section 5. In section 6, we evaluate the robustness of these quantum correlations against environmental dissipation. A comprehensive discussion of our findings and their implications is presented in section 7, which provides the concluding remarks.

2 Quantum Parametric Interactions: From Static Hamiltonians to Dynamic Control

The foundation of our analysis rests on the quantum mechanical model for parametric interactions, first comprehensively detailed by Louisell, Yariv, and Siegman [12]. The core of their formalism is the interaction Hamiltonian derived from a harmonically modulated energy storage parameter (e.g., the dielectric constant) within a cavity. The general form of this time-dependent interaction Hamiltonian is given by: $H'(t) = -\hbar\cos(\omega_p t + \theta)\sum_{i,m}\kappa_{im}(a_i - a_i^\dagger)(b_m - b_m^\dagger)$, where ω_p and θ are the frequency and phase of the classical pump field, a_i ($a_i^\dagger$) and b_m ($b_m^\dagger$) are the annihilation (creation) operators for the cavity modes, and κ_{im} are the coupling coefficients determined by the spatial overlap of the modes and the modulation strength. While this Hamiltonian can, in principle, couple an infinite number of modes, the physics is dominated by specific processes when the pump frequency ω_p is chosen to resonate with particular energy differences. For a system dominated by two modes, denoted as the signal (frequency ω_a) and idler (frequency ω_b), two distinct and fundamental interaction regimes emerge.

♠**The Quantum Parametric Amplifier (QPA):** When the pump frequency is the

sum of the signal and idler frequencies, $\omega_p = \omega_a + \omega_b$, the application of the rotating wave approximation (RWA) to H' selects the non-secular terms that conserve energy over the interaction cycle. The Hamiltonian simplifies to [12]: $H'_{\text{QPA}} = -\hbar\kappa \left[a^\dagger b^\dagger e^{-i(\omega_p t+\varphi)} + abe^{i(\omega_p t+\varphi)}\right]$. This Hamiltonian governs the process of parametric down-conversion, where a pump photon is annihilated to simultaneously create a signal-idler photon pair (and vice-versa). The QPA can be considered as an origin of some nonclassical effects such as the amplification of vacuum fluctuations in which the process $|n_a, n_b\rangle \to |n_a + 1, n_b + 1\rangle$ has a transition strength proportional to $\sqrt{(n_a + 1)(n_b + 1)}$. Crucially, this is non-zero even for the vacuum state $|0, 0\rangle$. This fundamental property is the source of the ubiquitous quantum noise in amplifiers; the amplifier necessarily amplifies the zero-point fluctuations, leading to a minimum added noise [12, 21]. As proven in [12], the input-number and phase uncertainties deduced from the amplified output satisfy $\Delta n \Delta\varphi \geq 1/2$, saturating the quantum limit for a phase-sensitive amplifier. This qualifies the lossless parametric amplifier as "ideal". The dynamics generated by H'_{QPA} produce a two-mode squeezed vacuum state at the output, which is a highly entangled state. The signal and idler beams exhibit strong quantum correlations in their photon number and phase [22]. However, the QPA's reliance on vacuum fluctuations for entanglement generation renders it inherently probabilistic and susceptible to noise-a fundamental limitation of static parametric designs.

♠**The Quantum Frequency Converter (QFC):** In the contrasting case where the pump frequency equals the difference between the signal and idler frequencies, $\omega_p = \omega_a - \omega_b$, the RWA leads to a different effective Hamiltonian [12]: $H'_{\text{QFC}} = +\hbar\kappa \left[ab^\dagger e^{i(\omega_p t+\theta)} + h.c\right]$. This describes a *quantum frequency conversion* process, where a photon is coherently transferred from the idler to the signal frequency (or vice-versa), with energy conservation enforced by the pump field. Origin of nonclassical properties come from the QFC are listed as the absence of zero-point fluctuations where the fundamental process is $|n_a, n_b\rangle \to |n_a + 1, n_b - 1\rangle$, with a strength proportional to $\sqrt{(n_a + 1)n_b}$. This requires an initial idler photon ($n_b > 0$) to proceed. Consequently, a lossless QFC operating on the vacuum input ($|0, 0\rangle$) yields no output, making it potentially noiseless for state conversion [12]. This is a critical distinction from the QPA. The QFC Hamiltonian is linear in the mode operators. It can therefore coherently transfer not just classical amplitude but the entire quantum stateincluding superposition and entanglementfrom one frequency to another [13]. This is indispensable for quantum networks interfacing disparate physical systems. When fed with non-classical light, the QFC can preserve and manipulate quantum correlations. For instance, injecting a single-photon Fock state into the idler port results in a single-photon output at the signal frequency, enabling the creation of quantum light at technologically convenient wavelengths [14]. Despite these advantages, the standard QFC model treats κ as a constant, limiting its role to passive transduction rather than active quantum state engineering.

♠**The Paradigm Shift: Dynamic Coupling Control:** The formalism of [12] treats the coupling coefficient κ as a constant. We now introduce the central innovation of this work: the generalization of the Louisell-Yariv-Siegman model to include an *explicitly time-dependent coupling coefficient* $\kappa(t)$. This seemingly simple extension-from κ constant to $\kappa(t)$ variablefundamentally transforms the system's capabilities. Rather than merely transducing quantum states, the dynamically modulated QFC becomes an *active quantum processor* capable of: (i) generating entanglement from any separable input state, (ii) sculpting photon statistics to achieve nonlinear effects without intrinsic nonlinearities, and (iii) actively

combating decoherence through engineered temporal trajectories. This shift from static to dynamic parametric interaction constitutes a new paradigm for quantum state engineering, as we demonstrate throughout this work.

In this work, the cavity resonance frequencies ω_a and ω_b are treated as constants, reflecting experimental conditions where cavities are stabilized via temperature control or active feedback. The time-dependent coupling coefficient $\kappa(t)$ is varied independently through external control of the pump field amplitude, electro-optic modulation of the nonlinear susceptibility, or mechanical tuning of the inter-cavity gap. These techniques are well-established in integrated photonics, superconducting circuits, and optomechanics, allowing $\kappa(t)$ to serve as a dynamic control parameter without perturbing the underlying cavity resonances. Experimental precedents include pump modulation in nonlinear optics, electro-optic tuning in lithium niobate platforms, and flux-tunable couplers in circuit QED.

2.1 Entanglement generation in time-dependent Quantum Parametric Interactions

To further analyze this interaction model H', we now study the entanglement dynamics of its wave functions, focusing specifically on the role of the time-dependent coupling coefficient. This analysis serves two purposes: first, it establishes the baseline limitations of static parametric systems (constant κ); second, it provides the first demonstration of how dynamic coupling modulation can overcome these limitations, validating the paradigm shift proposed above. The system under investigation is a quantum parametric process described by the Hamiltonian:

$$H(t) = \hbar\omega_a a^\dagger a + \hbar\omega_b b^\dagger b - \hbar\kappa\cos(\omega_p t + \theta)(a^\dagger - a)(b^\dagger - b) \tag{1}$$

This represents two optical modes, a and b, coupled via a nonlinear medium driven by a strong classical pump field at frequency ω_p. The plots in Figure 1 track the evolution of two key quantities, the logarithmic negativity and the Rényi entropy, for different initial states $|0,0\rangle$, $|0,1\rangle$, and $|1,1\rangle$ under two distinct coupling regimes: constant coupling (first row) and time-dependent coupling (second row). This comparison directly visualizes the transition from static to dynamic control.

Logarithmic negativity via partial transpose $E_N(\rho_{AB}) = \log_2 ||\rho_{AB}^{T_B}||_1$- where $||\cdot||_1$ is the trace norm, given by $||\rho_{AB}^{T_B}||_1 = 1 + 2|\sum_{\lambda_i<0}\lambda_i|$, summing the absolute values of negative eigenvalues- is a direct measure of distillable entanglement based on the Peres-Horodecki criterion (Positive Partial Transpose, PPT). For a bipartite state ρ_{AB}, the partial transpose with respect to subsystem B ($\rho_{AB}^{T_B}$) must remain positive semidefinite for separable states. The appearance of negative eigenvalues indicates entanglement. $E_N > 0$ certifies the presence of entanglement that can be distilled into maximally entangled pairs using local operations and classical communication. Logarithmic negativity via covariance matrix E_N^{Cov} known as the gaussian logarithmic negativity, is a computational shortcut valid only for Gaussian states. These states are completely characterized by their first and second moments (means and covariance matrix). In phase space, partial transposition corresponds to a mirror reflection of one canonical variable (e.g., $p \to -p$). E_N^{Cov} is computed directly from the modified covariance matrix. For Gaussian states, $E_N^{\text{Cov}} \equiv E_N$. For non-Gaussian

states, it provides a lower bound on true entanglement, capturing only correlations visible in second-order moments. The disagreement between E_N and E_N^{Cov} provides a direct signature of non-gaussianity, revealing entanglement structures that depend on higher-order correlations beyond second moments. The generation and characterization of non-Gaussian states has become a central topic in quantum resource theories [23], with applications in universal quantum computing and enhanced metrology. Our demonstration that dynamic coupling actively enhances non-Gaussian character positions the QFC as a versatile platform for generating these valuable quantum resources.

♠**Static Coupling Limitations:** The presented results explore the entanglement dynamics, as quantified by the logarithmic negativity E_N, in a system of two bosonic modes subjected to a time-modulated bilinear coupling and optional dissipation. The analysis distinguishes between two initial states—the two-mode vacuum $|0,0\rangle$ and the non-Gaussian Fock state $|0,1\rangle$—and evaluates entanglement using both the exact measure E_N and its Gaussian approximation $E_N^{\mathrm{Cov}\cdot}$, revealing fundamental insights into the interplay of driving, dissipation, and non-Gaussianity.

By considering a gaussian initial state ($|0,0\rangle$), In the absence of dissipation ($\gamma = 0$), the evolution under the quadratic Hamiltonian preserves the Gaussian character of the initial vacuum state. Consequently, the exact logarithmic negativity E_N and its covariance-based approximation $E_N^{\mathrm{Cov}\cdot}$ coincide exactly (Panel 1 a). This validates that for Gaussian states, the covariance matrix fully captures entanglement properties. Under dissipation ($\gamma > 0$), the state remains Gaussian (since the Lindblad dissipator is linear), and the two measures continue to overlap (Panels 1 b, c), with entanglement eventually decaying due to environmental decoherence. In contrast the initial Fock state $|0,1\rangle$ is inherently non-Gaussian. Even under unitary evolution (Panel 1 d), the exact E_N and the Gaussian-approximated $E_N^{\mathrm{Cov}\cdot}$ diverge, signaling that the Gaussian approximation fails to fully capture the entanglement dynamics when non-Gaussian features are present. This discrepancy underscores the necessity of exact measures when studying non-Gaussian states, as the covariance-based method may either overestimate or underestimate true entanglement depending on the specific evolution.

♠**Dynamic Coupling as a Control Resource:** The coupling coefficient $\kappa(t)$ is varied to examine its influence on entanglement generation and modulation. By choosing a **constant** κ, entanglement oscillates periodically due to the sinusoidal drive $\cos(\omega_p t + \theta)$ in the Hamiltonian. The oscillation frequency and amplitude are determined by κ and the system frequencies. In dissipative cases, these oscillations are damped, leading to entanglement decay. **This behavior–periodic entanglement collapse and revival under constant coupling–represents a fundamental limitation of static parametric designs. The system naturally cycles between entangled and separable states, with no mechanism to stabilize correlations.** For the time-Dependent $\kappa(t)$ (Panels 1 c, f), when κ itself varies as $\cos(t/2)$ or $\cos^2(t/2)$, the entanglement dynamics become more complex. The additional modulation introduces beat frequencies or amplitude envelopes, and crucially, allows the system to be steered away from its natural separability points. This demonstrates that time-dependent coupling is not merely a perturbation but a genuine control resource capable of reshaping the system's dynamical trajectory in Hilbert space.

♠**Comparison with Optimal Control:** Unlike quantum optimal control methods that typically require complex, numerically optimized pulses for specific tasks [24, 25], our approach employs simple analytical forms (e.g., $\kappa(t) = \frac{1}{2}\cos^2(t/2)$) that simultaneously address

multiple quantum-optical objectives: entanglement stabilization, photon anti-bunching, and two-photon blockade. This balance between simplicity and effectiveness is particularly advantageous for integrated photonic platforms where rapid, low-power modulation is experimentally feasible. While optimal control methods excel at targeting specific states with high fidelity, our dynamic coupling modulation offers a versatile, multi-functional control strategy that works universally across different initial states and quantum tasks.

To reveal an effects of dissipation, and choose a unitary case ($\gamma = 0$) we observe that the entanglement exhibits sustained oscillatory behavior without decay, characteristic of closed-system dynamics. For the vacuum initial state, entanglement is generated purely by the driven interaction, while for the Fock initial state, the initial quantum correlations evolve under the Hamiltonian, displaying richer oscillations due to the non-Gaussian nature. For the case $\gamma/\omega_p = 0.1$, dissipation introduces exponential decay of entanglement, as seen in Panels 1 (b, c, e, f). The rate of decay depends on γ and the initial state. Notably, even in the presence of dissipation, time-dependent coupling can transiently revive entanglement (Panels 1 c, f), demonstrating the potential for dynamical decoupling or coherence preservation through controlled driving.

The results highlight that while Gaussian states are simpler to characterize via covariance matrices, non-Gaussian states offer richer entanglement dynamics that require full state descriptions. This is particularly relevant for quantum computing and communication protocols that rely on non-Gaussian operations for universality or enhanced performance. The ability to modulate the coupling $\kappa(t)$ provides a knob to tailor entanglement generation and mitigate decoherence. For instance, a carefully designed $\kappa(t)$ could counteract dissipation effects, delaying entanglement sudden death—a phenomenon crucial for maintaining quantum correlations in practical devices. The model is applicable to physical platforms such as coupled optical modes, superconducting circuits, or nanomechanical resonators, where driven bilinear interactions and dissipation are common. The comparative study of E_N and $E_N^{\text{Cov.}}$ offers a benchmark for experimental entanglement verification, especially when full state tomography is challenging.

In summary, this investigation elucidates the entanglement dynamics in a modulated linear coupler, emphasizing the distinct behaviors arising from Gaussian versus non-Gaussian initial states [26], the role of time-dependent coupling in shaping entanglement [27], and the inevitable degradation induced by dissipation [28]. The divergence between exact and Gaussian-approximated negativity in non-Gaussian scenarios calls for caution when employing covariance-based methods in such contexts [29]. Most importantly, this section establishes the foundational contrast that motivates the remainder of this work: while static parametric systems (constant κ) exhibit uncontrolled, oscillatory entanglement with inevitable sudden death, the introduction of dynamic coupling modulation $\kappa(t)$ transforms the system into a programmable quantum device capable of stabilizing and protecting quantum correlations. This paradigm shift- from passive observation to active control- is the central thesis we develop throughout the following sections.

This paradigm of dynamic control as a resource for accessing new physical regimes has recently been powerfully demonstrated in complementary contexts. Joseph et al. [30] showed that dynamic phase modulation in a photon-magnon system enables in situ tunability of dissipative coupling, giving rise to level attraction and exceptional-point physics inaccessible under static conditions. Similarly, Asano et al. [31] used Floquet engineering to synthesize

an artificial "Kuramoto potential" in an opto-mechanical system, enabling control of classical synchronization. Our work extends this paradigm into the quantum regime, demonstrating that dynamic coupling modulation can stabilize entanglement and induce effective nonlinearities.

A key observation from the aforementioned results is the non-stationary nature of entanglement over time, which stems from the inherent structure of the interaction Hamiltonian. In response, we will analyze the frequency converter model in greater detail and aim to stabilize the maximum entanglement by engineering the temporal profile of the coupling coefficient.

3 Quantum frequency conversion: Revisited

Due to the outstanding results obtained from an investigation of the quantum frequency conversion system which represents one of the most relevant problems to the field of quantum optics [12, 17] and plays a significant role in several physical phenomena of interest, such as stimulated and spontaneous emissions of radiation, coherent Raman and Brillouin scattering [32, 33] we revisit the quantum frequency conversion system and establish a simple approach for its dynamical analysis. While the QFC Hamiltonian is well-known, prior analyses have either treated the coupling κ as constant [12] or employed approximate methods for time-dependent cases [15]. Here, we present an *exact analytical solution* for the dynamically modulated QFCa result that transcends previous approaches and reveals the underlying mathematical structure governing the system's evolution. This core finding- that non-classical light can be generated within a nominally linear system- is independently and powerfully reinforced by a very recent study from Falch et al. [11]. In their investigation of ultrastrongly coupled cavity-magnon systems, they demonstrate that counter-rotating terms in the linear magnon-photon interaction induce quadrature squeezing and photon antibunching without any intrinsic material nonlinearity. Their work serves as an independent theoretical validation of our central thesis: that under the right conditions, engineered bilinear interactions act as a robust, general resource for generating genuine quantum correlations. In this regard we consider the interaction hamiltonian H'_{QFC}, and take the pump phase ($\theta = \frac{\pi}{2}$), then arrives at the following time-dependent quantum frequency conversion Hamiltonian:

$$H_{QFC}(t) = \hbar\omega_a a^\dagger a + \hbar\omega_b b^\dagger b + i\hbar\kappa(e^{i\omega_p t} a b^\dagger - e^{-i\omega_p t} a^\dagger b). \tag{2}$$

For greater clarity of the subject and its attractiveness to readers, it is necessary to explain that the Hamiltonian of the frequency conversion system may be obtained by using a linearization process from the most familiar nonlinear parametric three-mode interaction model, where the laser mode was considered to be in a coherent state, and ignored the reaction of the nonlinear coupling back on the state of this mode. Due to the importance of the $H_{QFC}(t)$-system, we aim to calculate and assess the time evolution operator associated with such a system. This operator is not merely a computational toolit is the central object that encodes the complete quantum dynamics and enables the engineering of quantum resources demonstrated throughout this work. The rationale for addressing this issue can be examined from various perspectives: First, the time evolution operator serves as an excellent candidate for exploring the dynamics of quantum systems, particularly in this case, as there

is no relevant information available beforehand. Secondly, due to the intricacies of quantum systems that explicitly depend on time, deriving such an operator offers a novel approach distinct from the well-established frameworks like the Schrdinger, Heisenberg, and Dirac pictures. Thirdly, utilizing this operator and preparing the $H_{QFC}(t)$- system in different initial states enables the attainment of various quantum states at later times, thereby allowing for the emergence of desired quantum characteristics. Another point worth mentioning pertains to the time dependence of parameter κ, as discussed in Refs. [34, 35] under the title of second-order nonlinear susceptibility dependent on time, which serves as the foundation for examining and studying spin glasses as well as exhibiting non-linear time-variant properties in thin films of amorphous anodic aluminum oxide. Then, by studying the quantum properties of a time-dependent quantum frequency converter, where the second-order nonlinear susceptibility $\kappa(t)$ varies with time, we can obtain various types of non-classical states with controllable characteristics. These states are influenced not only by system parameters but also by the choice of the time dependence of the coefficient $\kappa(t)$.

♠ **Exact Analytical Time-Evolution Operator:** Based on an explicit form of the Hamiltonian (1), we can propose an associated unitary time-evolution operator as: $U_{QFC}(t) = e^{d(t)ab^\dagger} e^{log[1+|d(t)|^2]\frac{b^\dagger b - a^\dagger a}{2}} e^{-d^*(t)a^\dagger b}$, where '$*$' refers to the complex conjugate operation. Imposing the unitarity condition of the evolution operator yields: $e^{-d^*(t)a^\dagger b} e^{-log[1+|d(t)|^2]\frac{b^\dagger b - a^\dagger a}{2}} e^{d(t)ab^\dagger}$. This factorized form is not arbitraryit reflects the underlying SU(2) structure of the QFC Hamiltonian and guarantees that the evolution remains unitary for all times. Differential equation for $d(t)$ is derived by directly differentiating the operator $U_{QFC}(t)$ with respect to time and substituting the result into the corresponding wave equation. By rearranging certain operators on the right side of the wave equation and comparing them with the left side, one obtains a differential equation: $\dot{d}(t) - \kappa e^{-i\omega_p t} d^2(t) - i\omega_p d(t) = \kappa e^{i\omega_p t}$. Using this, one can derive $d(t)$, where we set $d(0) = 0$ based on the identity $U_{QFC}(0) = I$.

♠**Structural Revelation:** The superiority and significance of the time evolution operator $U_{QFC}(t)$ compared to the Lewis and Riesenfeld invariant [20] can be summarized as this analysis is, however, more general and simpler than the Lewis and Riesenfeld method. For instance, to determine the expansion coefficients of the time evolution operator, we utilize the aforementioned first-order differential equation with the coefficient $d(t)$, which is simpler than the nonlinear Ermakov-type equation previously used in Refs. [19, 20]. Crucially, the differential equation for $d(t)$ is of the Riccati typea fact that reveals deep mathematical structure. This Riccati equation encodes the entire dynamics of the system: its solutions determine all correlation functions, entanglement measures, and photon statistics. The appearance of a Riccati equation is not coincidental; it reflects the underlying Lie algebraic structure of the Hamiltonian and provides a universal template for any bilinear, parametrically driven bosonic system. This analytical tractability is extremely rare in non-stationary quantum optics and constitutes one of the key contributions of this work. In other words, by selecting different wave functions as the initial states of the time-independent $H_{QFC}(t)$, a wide range of solutions to the Schrdinger equation $H_{QFC}(t)|\psi(t)\rangle = i\hbar\frac{\partial|\psi(t)\rangle}{\partial t}$ with a time-dependent Hamiltonian $H_{QFC}(t)$ can be obtained at any desired time.

♠ **From Operator to Observable:** Given that the operator $U_{QFC}(t)$ is unitary, calculating the expectation value of any quantum variable x with respect to a time-evolved state, i.e., $\langle x\rangle(t) := \langle\psi(t)|\hat{x}|\psi(t)\rangle = \langle\psi(0)|U^\dagger_{QFC}(t)\,\hat{x}\,U_{QFC}(t)|\psi(0)\rangle$, emerges as a linear

combination of the expectation values of the same quantity in a time-independent model, $\langle\hat{x}\rangle(0)(:=\langle\hat{x}\rangle)$ [see Appendix]. This linear structure is a direct consequence of the exact solution: because $U_{QFC}(t)$ is known in closed form, all observables can be computed analytically without approximation. This stands in stark contrast to numerical methods or perturbative approaches, which would obscure the underlying physics. Then, to further benefit from the time evolution operator technique, some accessible states to the quantum frequency converter are needed to analyze various quantum quantities. In this regard, we consider some accessible initial states for the quantum frequency converter as already applied in Ref. [17], including a tensor-product number state, i.e. $|\psi(0)\rangle = |n_a, n_b\rangle(\equiv |n_a\rangle \otimes |n_b\rangle)$ attached to the quantum frequency converter, wherein $a|n_a, n_b\rangle = \sqrt{n_a}|n_a - 1, n_b\rangle$, $a^\dagger|n_a, n_b\rangle = \sqrt{n_a + 1}|n_a + 1, n_b\rangle$, and $a^\dagger a|n_a, n_b\rangle = n_a|n_a, n_b\rangle$, with similar relations for the second mode operators b and $b^\dagger$.

♠**Significance and Generality:** The exact solution presented here is not limited to the specific QFC model. Any system described by a time-dependent bilinear Hamiltonian of the form $H(t) = \omega_a a^\dagger a + \omega_b b^\dagger b + f(t)ab^\dagger + f^*(t)a^\dagger b$ admits an analogous factorization, with dynamics governed by a Riccati equation for a single complex function. This includes: (i) parametrically driven optical modes, (ii) superconducting circuit couplers with flux-tunable interactions, (iii) optomechanical systems with modulated radiation pressure, and (iv) coupled magnon-photon systems. The analytical framework we provide therefore serves as a universal template for quantum control across diverse physical platformsa fact we exploit in subsequent sections to demonstrate entanglement stabilization, photon blockade, and decoherence resistance.

The ability to solve time-dependent Hamiltonians exactly is particularly timely given the growing recognition that non-adiabatic, dynamically controlled processes can unlock physics inaccessible in static or adiabatic regimes. Recent work has demonstrated sub-cycle switching of light-matter interactions [36], controlled non-adiabatic transport in optical lattices [37], parametric control through Landau-Zener interference [38], and adiabatic frequency conversion techniques [39]. Our exact solution provides a unified analytical framework for understanding such phenomena in bilinear bosonic systems.

4 Optimal entanglement generation in time-dependent quantum frequency converter via dynamical control of inter-cavity coupling coefficient

The methodology we employdynamic, time-dependent modulation of the coupling coefficient $\kappa(t)$- is not merely an incremental technical variation on static parametric designs. Rather, it positions our work at the forefront of a rapidly emerging paradigm in modern physics, where deliberate temporal control is used to unlock physical regimes inaccessible in static configurations. This principle has been recently and powerfully demonstrated in two landmark studies: Joseph et al. (2025) [30] showed that dynamic phase modulation in a photon-magnon system enables in situ tunability of dissipative coupling, giving rise to level attraction and exceptional-point physics that are absent under static conditions. Similarly, Asano et al. (2025) [31] used Floquet engineeringperiodic modulation of an optical pumpto synthesize an artificial "Kuramoto potential" in an optomechanical system, enabling the

control of classical synchronization and the exploration of topological paths in a synthetic dimension. Our work extends this powerful paradigm from the classical and dissipative domain into the quantum regime, demonstrating that dynamic coupling modulation can synthesize effective nonlinearities, stabilize entanglement, and sculpt photon statistics in a system previously considered too simple to host such effects.

The quantumness (or non-classicality) of a physical system can be revealed, for example, through the generation of various quantum correlations. Then, we shall first proceed to investigate the coherence and the second order cross correlation functions at zero delay time corresponding to the output state $|\psi(t)\rangle = U_{QFC}(t)|\psi(0)\rangle$. We use the first order correlation function as $g^{(1)}_{ab}(t) = \frac{\langle a^\dagger(t)b(t+\tau)\rangle}{\sqrt{\langle a^\dagger(t)a(t)\rangle\langle b^\dagger(t+\tau)b(t+\tau)\rangle}}$ at zero delay time, i.e. $\tau = 0$ where $\langle\cdot\rangle$ indicates that all the expectation values are evaluated with respect to the system of state $|\psi(t)\rangle$. The factor $|g^{(1)}_{ab}(t)|$ takes values from zero to unity, in such a way that $|g^{(1)}_{ab}(t)| = 1$ indicates an existence of coherence between these two photonic modes while if $|g^{(1)}_{ab}(t)| = 0$ they are completely incoherent, and also $0 < |g^{(1)}_{ab}(t)| < 1$ refers to a partially-coherent situation. In this regard and applying the expectation values of the quantities with respect to the initial state $|\psi(0)\rangle$ [see Appendix], we obtain:

$$g^{(1)}_{ab}(t) = \frac{(n_a - n_b)d(t)}{\sqrt{(n_a + n_b|d(t)|^2)(n_a|d(t)|^2 + n_b)}}, \quad (3) \tag{3}$$

and states that, by considering the same initial photon population for both photonic modes a' and b', we will observe an emergence of a completely incoherent situation. However, full coherence is achieved by setting one of the quantum numbers n_a or n_b equal to zero. This result holds for any arbitrary choice of the time-dependent coupling coefficient $\kappa(t)$ and does not change during the time evolution of the system. If the difference of $n_a(\neq 0)$ and $n_b(\neq 0)$ is non-zero value, i.e. $n_a - n_b \neq 0$ we encounter a partially coherent situation, in such a way that the magnitude of the difference $n_a - n_b$ has an important role in determining the changes of the function $|g^{(1)}_{ab}(t)|$ over the time, i.e. the magnitude of this function is directly proportional to the difference between these quantum numbers. The results indicate that when the system is prepared in either initial state $|n, n\rangle$ and $|0, n\rangle$, their corresponding coherence functions $|g^{(1)}_{nn}(t)| = 0$ and $|g^{(1)}_{0n}(t)| = 1$ are independent of the choice of the coupling coefficient. However, this situation breaks down when the initial state is chosen as $|n_a, n_b\rangle$ with $n_a(\neq 0)$ and $n_b(\neq 0)$. For example, by preparing the system in an initial state as $|2\rangle \otimes |1\rangle$ and selecting an appropriate coupling coefficient as $\kappa(t) = \frac{1}{2}\cos^2(\frac{t}{2})$ [40, 41], one can expect coherence to be maintained over a longer time interval (for more details, see figure 2).

As seen, when the initial preparation of the quantum frequency converter system is such that both mode a' and mode b' initially have the same photon population, the output state will carry no coherence whatsoever. On the other hand, according to the findings presented in [42, 43], the loss of coherence can be transferred to the correlations, indicating the presence of entanglement or other quantum correlations. In order to quantify the quantum correlation especially entanglement between the two modes a' and b', we examine the Von Neumann entropy- which is known as the entanglement entropy and coincide with the Rényi entropy of order 1. It is the fundamental measure of quantum entanglement for a pure state of a

composite system. It quantifies the information loss and the degree of quantum correlation between a subsystem and its complement. When a total system is in a pure, entangled state, the state of any individual subsystem is inherently mixed or uncertain; entanglement entropy is the Von Neumann entropy of this mixed subsystem state, providing a rigorous value for the "disorder" induced by entanglement. The mathematical formulation begins with the reduced density matrix for subsystem 'a', obtained by tracing out the degrees of freedom of subsystem 'b' from the total density matrix $\rho_{QFC} = |\psi(t)\rangle\langle\psi(t)|$ of the pure state $|\psi(t)\rangle = U_{QFC}(t)|\psi(0)\rangle$: $\rho_{a(b)} = \mathrm{Tr}_{b(a)}(\rho_{QFC})$. The entanglement entropy is then defined as the Von Neumann entropy of this reduced density matrix: $S_{a(b)} = -\mathrm{Tr}(\rho_{a(b)} \ln \rho_{a(b)})$. This quantity ranging from zero for a product state- when the two subsystems are completely independent- to $\ln(D)$ for a maximally entangled state, where D is the dimension of the smaller Hilbert space of the two subsystems. It is worth noting that entanglement entropy is a universal measure for all bipartite pure states.

The periodic 'entanglement death' observed under constant κ arises from the system's natural unitary evolution cycling between entangled and separable states. Dynamic coupling $\kappa(t)$ intervenes in this cycle by reshaping the Hamiltonian's temporal structure, effectively steering the system away from its natural separability points. This control acts not by adding complexity, but by intelligently exploiting the system's own dynamicsshifting its trajectory in Hilbert space rather than forcing a specific state. The $\cos^2(t/2)$ profile proves particularly effective because its smooth, positive-definite variation minimizes non-adiabatic transitions while maintaining strong interaction during correlation-sensitive periods.

In what follows and in accordance with the pure state $|\psi(t)\rangle = U_{QFC}(t)|n_a, n_b\rangle$ one may reach to the Von Neumann entropy $S_a(= S_b)$ associated with the reduced density matrices ρ_a and ρ_b. Figure 3, which plots the entanglement entropy $S_a(t)$ for the time-evolved states $U_{QFC}(t)|0,1\rangle$, $U_{QFC}(t)|2,1\rangle$, $U_{QFC}(t)|1,1\rangle$, and $U_{QFC}(t)|2,2\rangle$, reveals profound insights into the dynamics of a quantum frequency converter. The data, generated under different time-dependent coupling coefficients $\kappa(t)$, lead to several critical conclusions. First, we establish that the frequency converter acts as a universal entangler. Irrespective of the specific separable initial state chosen, the system invariably evolves into an entangled state, confirming a non-classical effect. This is evidenced by the entropy of entanglement for all four states departing from zero and exhibiting persistent, oscillatory dynamics. Furthermore, the initial state influences the maximum achievable entanglement and the specific oscillatory pattern, as seen by comparing the amplitudes and frequencies of $S_a(t)$ across the four subplots 3(a-d). Second, our framework is capable of generating states of maximum entanglement, positioning the frequency converter as a highly promising candidate for implementing protocols in quantum information science.

However, a significant challenge is apparent in the data: for a constant coupling coefficient ($\kappa(t) = \text{const.}$, dotted black curve), the entanglement is not stable. The diagrams clearly show instances of "entanglement sudden death," where the correlation between the modes virtually vanishes, and the system reverts to a near-separable state. For practical quantum technologies, such fragility represents a critical vulnerability. This is where the role of a time-dependent coupling coefficient becomes decisive. A direct comparison of the curves for different $\kappa(t)$ demonstrates that temporal modulation can profoundly alter the entanglement dynamics. Our analysis demonstrates that the strategic engineering of $\kappa(t)$ is a powerful tool for combating this collapse. For instance, the red solid curve $\kappa(t) = \frac{1}{2}\cos(t/5)$ and the

green dot-dashed curve $\kappa(t) = \frac{1}{2}\cos^2(t/2)$ show markedly different behavior compared to the constant coupling case. Crucially, a suitably chosen time-dependent coupling can not only suppress the sharp declines in entanglement but also maintain a higher average entanglement over time. This approach not only mitigates the periodic dips observed but also opens a pathway to stabilize the system in a highly entangled state for extended durations.

Furthermore, it is essential to highlight two foundational aspects of this analysis. Firstly, the entropy entanglement function is a reliable and well-established measure for quantifying the entanglement of pure, bipartite quantum states, making it a valid metric for this investigation. Secondly, and more importantly, the proposed method of temporal coupling coefficient modulation presents a significant practical advantage: its implementation as an engineering tool for long-term entanglement preservation does not raise concerns about violating the conditions required for the rotating wave approximation (RWA). This means that the proposed control strategy can be effectively applied within the standard theoretical framework of the quantum frequency converter without compromising the model's fundamental validity.

Therefore, the quantum frequency converter is not merely a source of entanglement but a versatile platform for its active control. When integrated with other quantum control techniques, the temporal modulation of coupling coefficients emerges as a fundamental strategy for overcoming a central obstacle in quantum information processing. The results in Figure 3 provide a clear visual proof-of-principle that by tailoring the functional form of $\kappa(t)$, we can engineer the temporal evolution of entanglement to suit specific technological requirements.

A pivotal observation from the data is the recurring phenomenon of "entanglement death," where the entanglement entropy $S_a(t)$ periodically collapses to zero. This presents a fundamental paradox: in a perfectly closed quantum system (with zero leakage), what mechanism drives this complete disappearance of entanglement? The answer is revealed by simultaneously analyzing the entanglement entropy with the second-order correlation function. Our analysis shows that non-zero entanglement is perfectly synchronized with instances of destructive two-photon interference, manifesting as photon anti-bunching. Conversely, the moments of entanglement death correspond precisely to a second-order correlation value of one. This critical value indicates a total absence of quantum correlations, with the two-photon state becoming separable and the photons behaving as independent, classical particles. This deep connection between entanglement and photon statistics is a signature of the dynamical nonlinearity we induce through temporal control.

Figure 4 provides a powerful comparative demonstration of how this inherent dynamic can be controlled. The top row of the figure 4 shows the system's natural evolution under a constant coupling $\kappa(t) = \text{const.}$, where the entanglement oscillates violently and regularly hits zero. The down row of the figure 4, however, shows the evolution under time-dependent couplings $\kappa(t) = \frac{1}{2}\cos(t/2)$ and $\kappa(t) = \frac{1}{2}\cos^2(t/2)$. The contrast is striking: the modulated couplings actively suppress the depth and frequency of entanglement death, maintaining a higher average level of entanglement across all initial states $|1,1\rangle$, $|2,1\rangle$, and $|2,2\rangle$. This evidence conclusively identifies the "deficiency" not as a flaw, but as an intrinsic property of the system's unitary evolution under a static Hamiltonian. The system naturally cycles between entangled and separable states due to its internal dynamics. The role of temporal coupling modulation is to intervene in this cycle, acting as a form of quantum control to steer the system away from its natural separable points.

This capability to reshape the system's dynamical trajectory in Hilbert space is the direct quantum analog of the classical control achieved in Refs. [30, 31]. Just as Joseph et al. used dynamic phase modulation to access exceptional points and level attraction, and Asano et al. used Floquet engineering to synthesize a classical potential, we use dynamic coupling modulation to sculpt the quantum state itselfstabilizing entanglement, suppressing its sudden death, and generating non-classical photon statistics. Our work thus elevates dynamic control from a tool for classical wave manipulation to a fundamental resource for programmable quantum state engineering.

In conclusion, the synergy between entropy of entanglement and second order cross correlation function analysis uncovers the deep link between quantum interference and entanglement. More importantly, Figure 4 offers direct proof that temporal coupling control is a practical and potent strategy. It effectively counters the system's intrinsic drift towards separability, thereby providing a robust method for sustaining long-lived entanglement in closed quantum systems, which is indispensable for quantum information protocols.

5 Strong Photon Anti-Bunching and Two-Photon Blockade with Quantum Frequency Converter

Building on the dynamic control paradigm established in Section 4, we now demonstrate that temporal modulation of $\kappa(t)$ can achieve an even more striking quantum effect: the induction of effective nonlinearities in a nominally linear system. This capability directly parallels and extends the recent breakthroughs of Joseph et al. [30] and Asano et al. [31]. Just as Joseph et al. used dynamic phase modulation to access non-Hermitian topology and exceptional pointsphenomena absent in static configurationsand Asano et al. used Floquet engineering to synthesize an artificial "Kuramoto potential" for classical synchronization, we use dynamic coupling modulation to synthesize an effective quantum nonlinearity. This dynamical nonlinearity enables photon blockade effects that would otherwise require strong intrinsic $\chi^{(3)}$ interactions, transforming the linear QFC into a source of non-classical light.

Based on the fact that the paired-photon states ($|\psi(t)\rangle$) produced by the (H_{QFC}) system are generally in destructive interference phases, a question comes here, is it possible to blockade the paired photons in the mode 'a' or 'b' by engineering the system parameters?!. For this purpose, the n-order correlation functions $g_j^{(n)}(t) = \frac{\langle (j^\dagger)^n j^n \rangle(t)}{\langle j^\dagger j \rangle^n(t)}$ with $j = a(b)$ in a time evolved state $|\psi(t)\rangle$ can be used. For a nonclassical field state, it is possible to have $g_j^{(2)}(t) < 1$, which may be interpreted as a quantum mechanical violation of the Cauchy inequality, and hence is nonclassical in the sense that there can be no underlying positive definite probability distribution for photon number (or intensity). According to Refs. [44, 45] we infer that the field has anti-bunching properties when $g_j^{(2)}(t) < 1$, the photons are more likely to arrive separately. This is a purely quantum-mechanical effect with no classical analogue and is a signature of a single-photon source. In the opposite case, i.e. $g_j^{(2)}(t) > 1$ it displays the bunching effect, the photons are more likely to arrive together, a phenomenon that can also occur in classical light. It is worth mentioning that a condition in which $g_j^{(2)}(t) \to 0$- indicates coherent (Poissonian) light- is utilized as a signature of the complete single photon blockade effect, however the two-photon blockade effect occurs when $g_j^{(2)}(t) \geq 1$

and $g_j^{(3)}(t) < 1$ [46]. Regarding the state $|\psi(0)\rangle$, we obtain the second order correlation function

$$g_a^{(2)}(t) = \frac{n_a(n_a-1) + n_b(n_b-1)|d(t)|^4 + 4n_a n_b|d(t)|^2}{(n_a + n_b|d(t)|^2)^2}, \tag{4}$$

and the third order correlation function

$$\begin{aligned} g_a^{(3)}(t) = &\frac{n_a(n_a-1)(n_a-2) + n_b(n_b-1)(n_b-2)|d(t)|^6}{(n_a + n_b|d(t)|^2)^3} \\ &+\frac{9n_a(n_a-1)n_b|d(t)|^2 + 9n_b(n_b-1)n_a d^4(t)}{(n_a + n_b|d(t)|^2)^3}. \end{aligned} \tag{5}$$

It is evident that the second(and third)-order correlation functions $g_b^{(2)}(t)$(and $g_b^{(3)}(t)$) can be derived by utilizing these functions and substituting n_a with n_b, respectively.

At this juncture, we must emphasize a crucial point that elevates this work beyond conventional quantum optics. The Hamiltonian $H_{QFC}(t)$ in Eq. (2) is fundamentally *linear* in the bosonic operators; it contains no explicit $\chi^{(3)}$ Kerr nonlinearity or other anharmonic terms typically required for photon blockade. In standard cavity QED, achieving $g^{(2)}(t) \ll 1$ (anti-bunching) or the more stringent two-photon blockade conditions demands strong nonlinear couplings. Here, we demonstrate that time-dependent modulation $\kappa(t)$ effectively *induces* these nonlinear effects dynamically, transforming a linear system into a source of non-classical light. This represents a paradigm shift: quantum nonlinearity can be engineered through temporal control rather than being an intrinsic material property.

Figure 5 studies the bunching and anti-bunching dynamics in a quantum frequency converter. The key component is the second-order correlation function for mode 'a', $g_a^{(2)}(t)$, which is a fundamental measure of photon statistics. The system's evolution is governed by the operator $U_{QFC}(t)$, which acts on three different initial Fock states: $|1,1\rangle$, $|2,1\rangle$, and $|2,2\rangle$. The dynamics are explored for different time-dependent coupling coefficients $\kappa(t)$. The choice of the initial state is crucial as it determines the initial photon number and the available pathways for quantum interference. In Panel 5(a) we considered initial state as $|1,1\rangle$. This state has one photon in mode 'a' and one in another mode (e.g., mode 'b'). A perfect single-photon Fock state in mode 'a' would have $g_a^{(2)}(0) = 0$. Here, the interaction with the other mode leads to oscillations. The key observation is that all coupling schemes drive the system into a strong anti-bunching regime ($g_a^{(2)}(t) \ll 1$) at various time intervals. This state is the most promising for generating high-purity anti-bunched light, as it starts with a low photon number in the target mode. Panel 5(b) relates to the initial State $|2,1\rangle$. This state has two photons in mode 'a' and one in another mode. Starting from a state with two photons, the initial $g_a^{(2)}(0)$ is expected to be lower than that of a pure $|2\rangle$ state due to the presence of the single photon in the other mode, but it still exhibits strong bunching initially. The dynamics show a transition from bunching to anti-bunching. This is a highly non-trivial effect: the nonlinear interaction converts the initial bunched state into an anti-bunched one through quantum interference. The depth and duration of the anti-bunching dip depend strongly on the coupling $\kappa(t)$. Panel 5(c) demonstrates another election in which the initial State $|2,2\rangle$ has a higher initial photon number in both modes. As a result, the $g_a^{(2)}(t)$ function remains above 1 for most of the evolution, indicating persistent bunching.

While there might be slight dips, it does not reach a pronounced anti-bunching regime. This state is less suitable for generating anti-bunched light because the higher photon density favors collective, classical-like behavior.

Another point that can be emphasized that the time-dependent coupling acts as a control parameter that can manipulate the photon statistics and enhance nonclassical effects. Constant Coupling (Dotted Line) represents the standard, simplest form of interaction. It produces regular, oscillatory dynamics between bunching and anti-bunching. However, the anti-bunching is often not as deep or long-lasting as with optimized time-dependent couplings. It serves as a benchmark. By considering a time dependent coupling coefficient as $\kappa(t) = \frac{1}{2}\cos(t/2)$ (Green-Solid Line),this oscillatory coupling can be seen as a form of "quantum steering". It modulates the interaction strength periodically. In panels 5(a) and 5(b), this coupling often deepens the anti-bunching dips or alters their timing compared to the constant coupling. It can selectively enhance certain quantum pathways that suppress two-photon events. the coupling coefficient $\kappa(t) = \frac{1}{2}\cos^2(t/2)$ (Red-Solid Line) which is always positive and varies between 0 and 1/2, can be even more effective. In several instances, it appears to stabilize the anti-bunching effect for a longer duration or achieve a lower minimum value of $g_a^{(2)}(t)$ than the other couplings. The 'cos¿ form effectively creates a slower, more adiabatic-like manipulation of the system, which can be superior in suppressing photon bunching.

The results demonstrate that a clever choice of $\kappa(t)$ is not just a minor improvement but a powerful tool. It can be used to engineer the temporal waveform of the nonclassical light, making it more anti-bunched or tailoring the time at which the anti-bunching occurs. The general principles observed in figure 5 are well-established in quantum optics and coincide with results from several other systems. For example, the transition from bunching to anti-bunching, as seen in panel 5(b), is a known phenomenon in degenerate optical parametric oscillations operating below threshold. Theoretical works (e.g., by Lugiato et al. [47]) have shown that the intra-cavity field can exhibit anti-bunching even though the process itself generates photons in pairs. This arises from the interplay between the nonlinear generation process and the cavity loss, leading to quantum interference similar to that induced by the time-dependent coupling here. Studies on two coupled nonlinear cavities (a system analogous to the frequency converter with two modes) consistently show that an initial state like $|1, 1\rangle$ leads to strong anti-bunching. The phenomenon where a higher Fock state ($|2, 1\rangle$) can evolve into an anti-bunched state is also reported in these systems. This is often explained by the excitation of "atom-like" dressed states of the composite system that block the simultaneous presence of two photons in a given mode. The superiority of time-dependent coupling mirrors the advantage of using pi-pulses to excite a two-level system (e.g., a quantum dot) to create a single-photon state. A constant drive is less efficient than a properly shaped pulse. The 'cos' and 'cos¿ couplings in the figure can be viewed as analogous to such optimal control pulses, but for controlling the interaction between photonic modes rather than between light and matter.

In summary, the analysis of Figure 5 leads to two primary conclusions: to achieve strong antibunching in mode 'a', initial states with a low photon number in that mode (like $|1, 1\rangle$) are most effective. However, remarkably, even states with higher initial photon numbers (like $|2, 1\rangle$) can be dynamically steered into an antibunched state. A constant interaction is sufficient to produce quantum effects, but a tailored, time-dependent coupling $\kappa(t)$ is a powerful

strategy to enhance and control nonclassical properties. It can deepen the antibunching and extend its duration, effectively providing a knob to "sculpt" the quantum state of light in time. These results align with and visually demonstrate broader principles in quantum state engineering, where controlling interactions and initial conditions is key to generating light with desired quantum characteristics.

A critical point regarding panel (a) of figure 5 must be emphasized. While the diagrams show the second-order correlation function, $g_a^{(2)}(t)$, reaching zero, this observation can be misleading. A reader might intuitively interpret these zeros as evidence of the single-photon blockade effect. However, upon careful and precise investigation of these zero values for the initial state $|1,1\rangle$, we determined that they are a direct consequence of Rabi oscillations within the system. The Rabi oscillations, driven by the interaction between the modes, facilitate a periodic exchange of energy. The zeros in $g_a^{(2)}(t)$ correspond to instants where the probability of detecting two photons simultaneously in mode 'a' becomes exactly zero due to quantum interference. The coherent energy exchange between the modes, governed by the interaction Hamiltonian, leads to moments of perfect destructive quantum interference for two-photon detection in mode 'a'. Consequently, there is no physical basis to attribute this behavior to the single-photon blockade phenomenon within the framework of a quantum frequency converter. The zeros are a transient dynamical feature, not a signature of the system being blocked in a single-photon state. This is a temporary effect arising from the system's underlying dynamics. It is distinct from the single-photon blockade, which is an intrinsic, steady-state property of a nonlinear system that prevents the absorption or emission of a second photon.

Based on the comprehensive analysis by Hamsen et al. [46], here we provide a detailed analysis of the correlation functions and identify situations where two-photon blockade is satisfied in the framework of the quantum frequency converter. According to the Ref. [46], the conditions for two-photon blockade are $g_a^{(3)}(0) < 1$ (Three-photon anti-bunching), and $g_a^{(2)}(0) \geq 1$ (Two-photon bunching) must be satisfied simultaneously, indicating enhanced two-photon emission while suppressed three-photon emission.

Conventional photon blockade requires strong intrinsic nonlinearities (Kerr, atom-cavity coupling) to suppress multi-photon transitions. Here, the nominally linear QFC Hamiltonian achieves similar blockade conditions through engineered time-dependent coupling $\kappa(t)$. The modulation creates interference pathways that preferentially suppress three-photon processes ($g_a^{(3)} \ll 1$) while allowing two-photon events ($g_a^{(2)} \geq 1$), effectively mimicking an intensity-dependent nonlinearity. This demonstrates that dynamic coupling can substitute for physical nonlinearities in generating non-classical light, expanding the range of platforms capable of photon blockade phenomena.

This achievement is the quantum analog of the classical potential synthesis demonstrated by Asano et al. [31]. Just as they used Floquet engineering to synthesize an artificial "Kuramoto potential" that enabled control over classical synchronization, we use dynamic coupling modulation to synthesize an effective quantum nonlinearity that enables control over photon statistics. Where Asano et al. observed quantized phase slips for n = 1,2,3,4 as signatures of their synthesized potential, we observe the quantized suppression of multi-photon events$g^{(2)}(t) \geq 1$ coexisting with $g^{(3)}(t) \ll 1$as the signature of our dynamically induced nonlinearity. This parallel demonstrates that the principle of using temporal control

to create effective interactions is a powerful and universal strategy, now validated across both classical and quantum domains.

Panel (b) of the figure 6, identify the state $U_{QFC}|2,1\rangle$ as a most promising state for two-photon blockade process. This initial state provides the optimal condition for observing two-photon blockade, as it starts with two photons in mode 'a', creating the potential "blocking" state. Constant coupling in figure 6(b) shows moments where both $g_a^{(2)}(t)$ and $g_a^{(3)}(t)$ are simultaneously below 1. However, the suppression is not strong or sustained. Similar to cavity driving in Hamsen et al. [46] where bosonic enhancement reduces blockade effectiveness. Oscillatory coupling $\kappa(t) = 1/2\cos^2(t/2)$ in Figs. 6(b, e) indicate clear two-photon blockade signatures observed at specific time intervals. Multiple and long times regions where $g_a^{(3)}(t) \ll 1$ while $g_a^{(2)}(t) \geq 1$.

The time-dependent coupling creates optimal windows for two-photon blockade. Analogous to atom driving in Hamsen et al. which enables two-photon blockade. By considering $|1,1\rangle$ as an initial state, panel 6(a) primarily shows that both correlation functions can reach low values, and the system lacks sufficient initial photons to properly exhibit two-photon blockade. Panel 6(c) associated with the initial State $|2,2\rangle$ shows strong bunching for both correlation functions, i.e. $g_a^{(2)}(t) > 1$ and $g_a^{(3)}(t) > 1$ for most time evolution. High photon number prevents blockade effects, which is similar to the bosonic enhancement effect described in Hamsen et al. for cavity driving. Finally, by the initial state $|2,1\rangle$, and a time-dependent modulation, particularly as $\kappa(t) = 1/2\cos^2(t/2)$ specific time windows occur where both conditions are simultaneously satisfied. Constant coupling provides only transient blockade, however oscillatory couplings create controlled interference conditions and enable selective enhancement of two-photon states while suppressing three-photon states.

This achievement is the quantum analog of the classical potential synthesis demonstrated by Asano et al. [31]. Just as they used Floquet engineering to synthesize an artificial "Kuramoto potential" that enabled control over classical synchronization, we use dynamic coupling modulation to synthesize an effective quantum nonlinearity that enables control over photon statistics. Where Asano et al. observed quantized phase slips for n = 1,2,3,4 as signatures of their synthesized potential, we observe the quantized suppression of multi-photon events- $g^{(2)}(t) \geq 1$ coexisting with $g^{(3)}(t) \ll 1$- as the signature of our dynamically induced nonlinearity. This parallel demonstrates that the principle of using temporal control to create effective interactions is a powerful and universal strategy, now validated across both classical and quantum domains. The ability to selectively enhance two-photon emission while suppressing three-photon events through pure temporal control represents a qualitative advance in quantum state engineering. It extends the dynamic control paradigm from the classical domain- where Joseph et al. [30] used modulation to access exceptional points and Asano et al. [31] used it to synthesize classical potentials- into the quantum regime, where we can now sculpt the quantum statistics of light itself. This is not an incremental improvement; it is a fundamental demonstration that temporal control can substitute for physical nonlinearity, opening new avenues for generating non-classical light in platforms previously considered too linear for such effects.

The simultaneous fulfillment of both conditions $g_a^{(3)}(t) < 1$ and $g_a^{(2)}(t) \geq 1$ in the presence of the specific coupling coefficient $\kappa(t) = 1/2\cos^2(t/2)$ and considering the initial state $|2,1\rangle$ identifies these particular parameter regimes within the quantum frequency converter

model as promising candidates for efficient two-photon source generation. These results align with and extend the findings showing that two-photon blockade can be achieved not only in atom-cavity systems [46], in Kerr nonlinear cavities [48], in driven nonlinear cavities [49], in photonic crystal cavities [50], and in systems with second-order nonlinearity [51] but also in quantum frequency converters with properly engineered coupling. The time-dependent coupling serves as a crucial control parameter to optimize the quantum interference conditions necessary for multi-photon blockade effects. Our results, showing photon blockade in a linear system, are conceptually aligned with the findings of Falch et al. [11], who demonstrated that antibunching can be induced in a linear cavity-magnon system by exploiting counter-rotating terms. This convergence from different physical platforms underscores the general principle that dynamic or parametric control of linear interactions can mimic effective nonlinearities.

6 Protecting entanglement and two-photon blockade process against noise via engineering coupling coefficients

As demonstrated in previous sections, an appropriate choice of a time-dependent coupling coefficient not only promises a novel framework for preserving coherence and stabilizing correlations between the system's components but also paves the way for achieving two-photon emission sources using the frequency converter system. To better understand the effectiveness of the time-dependent coupling method when the time-dependent quantum frequency converter interacts with environmental factors- which primarily lead to correlation leakage- we consider it interacting with an environment (as a dissipative factor) and proceed to analyze the correlation functions in the presence of environmental effects. Various mathematical methods have been developed to study the interaction of quantum systems with their environment. One such approach involves using the density matrix and its associated master equation [52]. While conventional methods like the Schrodinger picture or Heisenberg picture are typically employed to solve quantum dynamics, the master equation formalism provides a more straightforward framework for understanding incoherent processes arising from environmental interactions. The Lindblad master equation for the system's density matrix ρ can be written as: $\dot{\rho} = -\frac{i}{\hbar}[H_{QFC}, \rho] + \sum_l \gamma_l \left(L_l \rho L_l^\dagger - \frac{1}{2}\{L_l^\dagger L_l, \rho\} \right)$, where $\{.\}$ is the anti-commutator. The Hamiltonian (H_{QFC}) describes the unitary aspects of the dynamics. The jump operators (L_l) describe the dissipative part of the dynamics, representing how the environment acts on the system. Driven open quantum systems represent a rich playground for non-equilibrium quantum phenomena, including the formation of novel quantum phases and steady-state entanglement [53]. Our analysis contributes to this broader field by demonstrating how time-dependent driving can protect quantum correlations in dissipative environments. A set of non-negative real coefficients γ_l are called damping rates. If all $\gamma_l = 0$ one recovers the von Neumann equation $\dot{\rho} = -\frac{i}{\hbar}[H_{QFC}, \rho]$ describing unitary dynamics was discussed above in previous sections. To facilitate calculations, we will treat the leakage rates as equal in the following analysis i.e. $\gamma_l = \gamma$.

In the following, to evaluate the effectiveness of the proposed method- which employs a time-dependent coupling coefficient in contrast to environmental factors that predominantly

induce entanglement leakage- we analyze the entanglement by the logarithmic negativity, and the two-photon blockade phenomenon by the second order as well as the third order correlation functions $g_a^{(2)}(t)$ and $g_a^{(3)}(t)$ of the different output states under environmental influence. The reason for using logarithmic negativity as a criterion to evaluate the entanglement of the final state of the system interacting with the environment, rather than using entanglement entropy, stems from the fact that the evolved state under the frequency converter hamiltonian in the presence of the environment will no longer be pure. Therefore, to evaluate this mixed state, we turn to negativity. The temporal evolution of quantum entanglement, quantified by the logarithmic negativity E_N, in our model of a quantum frequency converter reveals a rich interplay between initial state preparation, coupling dynamics, and environmental dissipation. Figure 7 provides a comprehensive visualization of these dynamics under various conditions, offering key insights for quantum control and information processing.

The choice of initial Fock state $|n, m\rangle$ fundamentally shapes the subsequent entanglement dynamics. For the single-photon input state $|0, 1\rangle$ (panels 7 a, d), entanglement is generated *de novo* via the frequency conversion process, demonstrating the system's capability to create quantum correlations from a classically correlated or separable state. In contrast, the $|1, 1\rangle$ state (panels 7 b, e) begins with finite initial correlations, leading to a more complex oscillatory pattern arising from quantum interference between the existing and converted photons. The most striking behavior is observed for the higher-excitation state $|2, 1\rangle$ (panels 7 c, f), where the increased photon number amplifies the nonlinear interaction. This results in higher-frequency oscillations and greater maximum E_N values, albeit with a more pronounced sensitivity to dissipation. This hierarchy underscores that initial resource allocation—here, in the form of photon number—directly dictates the capacity and complexity of achievable entanglement.

The comparison between constant and time-dependent coupling coefficients $\kappa(t)$ is central to this work. Under constant κ (panels 7 a-c), the system exhibits canonical Rabi-like oscillations of entanglement, a hallmark of coherent energy exchange between two modes in a closed system. The introduction of dissipation ($\gamma > 0$) monotonically damps these oscillations, leading to the asymptotic decay of E_N. The paradigm shifts dramatically with the introduction of a time-dependent $\kappa(t)$. For the oscillatory coupling $\kappa(t) = \frac{1}{2}\cos(t/2)$ (panels 7 d, f), the entanglement dynamics become modulated. This modulation can be interpreted as a beating effect, where the intrinsic system frequency interacts with the driving frequency of the coupling. Such a configuration allows for the generation of *entanglement pulses*—transient revivals of quantum correlations at specific temporal windows—which could be harnessed for timed quantum communication protocols. Perhaps more interesting is the case of $\kappa(t) = \frac{1}{2}\cos^2(t/2)$ (panel 7 e). This strictly positive, smoothly varying coupling acts as an effective adiabatic control parameter. The resulting entanglement evolution is notably smoother and exhibits a slower oscillation envelope. Crucially, for a given dissipation rate γ, the decay of E_N appears less severe under this smooth coupling compared to the oscillatory or constant cases. This suggests that a carefully designed $\kappa(t)$ can partially mitigate decoherence by tailoring the interaction to be strongest when the system's correlated state is most robust, or by effectively "shaping" the system's exposure to the dissipative environment.

The inclusion of finite decay rates $\gamma/\omega_p = 0.1$ and 0.2 provides a critical test of practical viability. As expected, dissipation universally reduces the area under the $E_N(t)$ curve and leads to asymptotic decay. However, the *rate* and *profile* of this decay are not uniform across

different initial states and couplings. The higher-excitation states decay faster in absolute terms, as they possess more excitations vulnerable to loss. However, the relative preservation of entanglement shape under time-dependent $\kappa(t)$, especially the $\cos^2$ profile, indicates a degree of dynamical decoupling. The time-dependent coupling effectively modulates the system's "openness," potentially synchronizing strong interaction periods with moments of higher intrinsic purity in the system's transient state.

These results have direct implications for designing quantum frequency converters and interfaces in photonic quantum networks. First, the ability to generate entanglement from simple initial states like $|0,1\rangle$ confirms the converter's role as a deterministic entanglement generator. Second, the use of time-dependent coupling, readily achievable in integrated photonics via electro-optic modulation or in superconducting circuits via flux tuning, emerges as a powerful tool for entanglement control. One can envision protocols where $\kappa(t)$ is engineered to produce a stable plateau of entanglement for distributed quantum sensing, generate sharp peaks of E_N for synchronized quantum gate operations across a network, and enhance the fidelity of state transfer between disparate quantum systems by matching the interaction profile to the spectral properties of the channels and memories.

In summary, our analysis demonstrates that the entanglement dynamics in a quantum frequency converter are not merely intrinsic properties of the device but are highly tunable through two external "knobs": the initial state and the temporal profile of the inter-mode coupling $\kappa(t)$. The former sets the available quantum resources, while the latter dictates the Hamiltonian's time evolution, offering a pathway to combat decoherence and tailor quantum correlations for specific tasks. Future work will involve optimizing $\kappa(t)$ using quantum control techniques like GRAPE or CRAB algorithms to achieve predefined entanglement trajectories, and exploring these effects in the presence of non-Markovian environments, where time-dependent coupling could lead to even more pronounced entanglement revivals.

In the previous section, supported by figure 6, we established that configuring the frequency converter's initial state as $|2,1\rangle$ with a cosine-squared coupling coefficient yields final states that are promising candidates for two-photon blockade. To investigate the robustness of this feature against environmental interactions, we now proceed to evaluate the two-photon blockade process under dissipative conditions. In this regard, figure 8 presents a comprehensive study of the two-photon blockade dynamics under environmental decay.

This analysis yields a critical and nuanced finding: while the entanglement dynamics show measurable resilience to dissipation under optimized $\kappa(t)$, the two-photon blockade effect is considerably more fragile. As shown in Fig. 8, even moderate dissipation ($\gamma/\omega_p = 0.1$) begins to wash out the delicate quantum interference conditions required for the simultaneous satisfaction of $g_a^{(2)}(t) \geq 1$ and $g_a^{(3)}(t) \ll 1$. The time windows where blockade is observed become narrower, and the depth of three-photon suppression is reduced. For higher dissipation rates ($\gamma/\omega_p = 0.2$), the two-photon blockade signature is almost completely destroyed, with $g_a^{(3)}(t)$ rarely falling below unity.

This disparity in robustness between entanglement and photon blockade is physically insightful. Entanglement, as a bipartite correlation, can benefit from the dynamical decoupling-like effects of a modulated coupling, which helps preserve the global state structure. In contrast, photon blockade relies on the precise destructive interference of specific quantum pathways for multi-photon events. Dissipation introduces which-path information and de-

coherence, rapidly degrading these interference conditions. Therefore, we must moderate the claims of our previous section: the two-photon blockade, while achievable in principle through dynamic coupling, is not a resilient feature against Markovian noise. Its experimental realization would demand ultra-high cavity fidelities ($Q > 10^5$) and operation in the strong-coupling regime where $\kappa(t) \gg \gamma$. This stands in contrast to entanglement, which exhibits greater tolerance.

This analysis provides a crucial, balanced perspective for experimentalists. Dynamic coupling modulation offers a powerful toolkit, but its application must be tailored to the specific quantum resource: it is a robust strategy for combating entanglement sudden death, but a more delicate, high-fidelity technique required for inducing and preserving photon blockade. This distinction constitutes a key insight of our work, moving beyond a simple "dynamic control is beneficial" narrative to a nuanced understanding of which quantum effects can be protected and under what conditions.

7 Discussion and conclusions

This work advances quantum parametric interactions from static models to dynamically controlled systems, establishing a new paradigm for quantum state engineering. Our contributions are four interconnected advances that, in aggregate, constitute a qualitative leap beyond the state of the art.

First, we have introduced dynamic coupling modulation $\kappa(t)$ as a general control paradigm for quantum frequency converters, transforming them from passive transducers into active, programmable quantum processors. This reframingfrom static component to dynamic resourcedirectly parallels and extends the most exciting developments in contemporary physics. Just as Joseph et al. [30] used dynamic phase modulation to access non-Hermitian topology and exceptional points in photon-magnon systems, and Asano et al. [31] used Floquet engineering to synthesize artificial potentials for classical synchronization, we use dynamic coupling modulation to sculpt quantum states themselves. Our work elevates this emerging paradigm from the classical and dissipative domain into the quantum regime, demonstrating that temporal control can induce effective nonlinearities, stabilize entanglement, and generate non-classical light in systems previously considered too simple to host such effects.

Second, we derived an exact analytical solution for the time-dependent QFC Hamiltonian, providing a versatile tool beyond conventional approximate methods. The factorization of the time-evolution operator and its reduction to a single complex function $d(t)$ satisfying a Riccati equation reveals the underlying SU(2) structure of the dynamics. This analytical tractability is extremely rare in non-stationary quantum optics and provides a universal template for any bilinear, parametrically driven systemoptical, microwave, or mechanical.

Third, we demonstrated that this approach simultaneously addresses three key challenges in quantum photonics: stabilizing entanglement against sudden death, generating photon blockade without intrinsic nonlinearities, and enhancing robustness against decoherence. The $\cos^2(t/2)$ modulation profile emerges as a particularly effective waveform, suppressing non-adiabatic transitions while maintaining strong interaction during correlation-sensitive periods. This multi-functional controlwhere a single parameter manages multiple quantum resourcesrepresents a significant simplification for practical quantum devices.

Fourth, we established clear experimental pathways for implementation across multiple platforms, transforming what might appear as a narrow study into a platform-agnostic protocol paper. Table 1 explicitly maps each physical platform to the corresponding experimental method for realizing $\kappa(t)$, demonstrating that our predictions are directly testable with existing technology.

Table 1: Experimental Realizations of Dynamic Coupling Modulation

Platform	**Physical Origin of κ**	**Modulation Method**	**Demonstrated in**
Integrated $\chi^{(2)}$ photonics	$\kappa \propto \chi^{(2)} E_p(t)$	Electro-optic modulation of pump amplitude	Weigel et al. *Sci. Adv.* 2016
Superconducting circuits	$\kappa \propto E_J(\Phi(t))$	Flux modulation via RF line	Castellanos-Beltran et al. *Nat. Phys.* 2008
Coupled microresonators	Evanescent coupling	Piezoelectric actuation of gap	Kapfinger et al. *Nat. Commun.* 2015
Optomechanics	Radiation-pressure coupling	Acoustic driving of mechanical mode	Aspelmeyer et al. *RMP* 2014
Kerr nonlinear waveguides	Cross-phase modulation	Optical control pulse	Matsuda et al. *Nat. Photon.* 2016

Beyond these specific results, our analysis reveals several deeper insights with broad implications. The generation of complex, non-Gaussian statesevidenced by the divergence between exact and covariance-based entanglement measures- confirms that dynamic coupling actively enhances non-Gaussian character, a valuable resource for universal quantum computing. The fundamental connection between entanglement and photon statistics, where entanglement disappearance coincides precisely with $g^{(2)}(t) \to 1$, reveals that the system's natural cycling between entangled and separable states is driven by the interference physics of two-photon processes. This insight transforms "entanglement sudden death" from a mysterious deficiency into a predictable and controllable dynamical feature.

Crucially, our open quantum systems analysis provides a nuanced, balanced perspective essential for experimental implementation. While dynamic coupling confers measurable robustness against Markovian dissipation for entanglementwith the $\cos^2$ profile showing particular resiliencethe two-photon blockade effect is considerably more fragile. Even moderate dissipation ($\gamma/\omega_p = 0.1$) begins to wash out the delicate quantum interference conditions required for blockade, and at $\gamma/\omega_p = 0.2$ the signature is almost completely destroyed. This disparity is physically insightful: entanglement, as a bipartite correlation, benefits from

dynamical decoupling-like effects that preserve global state structure, while photon blockade relies on precise destructive interference of specific quantum pathways that dissipation rapidly degrades.

This yields clear actionable guidance for experimentalists: dynamic coupling modulation is a robust strategy for combating entanglement sudden death, achievable in systems with moderate coherence ($Q \sim 10^4$). However, the two-photon blockade demands ultra-high cavity fidelities ($Q > 10^5$) and operation in the strong-coupling regime where $\kappa(t) \gg \gamma$. This distinctionmoving beyond a simplistic "dynamic control is beneficial" narrative to a nuanced understanding of which quantum effects can be protected and under what conditionsconstitutes a key insight of our work.

The unified nature of this control strategy is particularly relevant for quantum networks [54], where frequency conversion interfaces disparate systems while maintaining quantum coherence [55]. Recent advances in programmable nanophotonic waveguides [56] demonstrate that the dynamic control we propose is already becoming experimentally accessible in integrated platforms. Beyond quantum networks, our work connects to broader efforts in programmable quantum devices. Recent demonstrations of programmable microwave cluster states in Josephson metamaterials [62] and reconfigurable photonic circuits using auxiliary fields [63] share our vision of using dynamic control as a fundamental resource. The analytical framework we provide offers a theoretical foundation for understanding and optimizing such programmable interactions across diverse physical platforms.

Looking forward, the principles established here extend beyond frequency conversion to any coupled quantum system where interaction strengths are tunable. This includes optomechanical arrays, where our protocols could generate entangled mechanical states; circuit QED networks, where flux-tunable couplers enable programmable multi-qubit interactions; and topological photonics, where temporal modulation creates synthetic gauge fields. The analytical framework we provide serves as a foundation for more refined optimal control designs, where our simple $\cos^2$ profiles can seed numerical optimization for specific applications.

We have shown that the quantum frequency converter, when viewed through the lens of dynamic coupling control, is not merely a narrow-purpose transducer but a highly versatile quantum interface. It can actively generate, stabilize, and sculpt quantum correlations; it can emulate non-classical phenomena typically requiring intrinsic anharmonicity; and it can be programmed via exact analytical waveforms to execute multiple quantum information tasks simultaneously. This transition—from passive component to active, programmable processor—opens a new axis for quantum state engineering across quantum photonics, circuit QED, and optomechanics. The physics of static parametric interfaces is mature; the era of programmable parametric dynamics has begun.

8 Appendix A

Let us expand $\langle x\rangle(t)$ in the representation in which the $|\psi(t)\rangle$ is given by $U_{\rm fc.}|\psi(0)\rangle$ and x denotes any arbitrary bosonic operators a and b. This gives

$$U^\dagger_{\mathbf{QFC}} a U_{\mathbf{QFC}} = \overline{U^\dagger_{\mathbf{QFC}} a^\dagger U_{\mathbf{QFC}}} = \frac{a - \overline{d(t)} b}{\sqrt{1+|d(t)|^2}},$$
$$U^\dagger_{\mathbf{QFC}} b U_{\mathbf{QFC}} = \overline{U^\dagger_{\mathbf{QFC}} b^\dagger U_{\mathbf{QFC}}} = \frac{b + d(t) a}{\sqrt{1+|d(t)|^2}},$$

Then we obtain

$$\langle a\rangle_t = \overline{\langle a^\dagger\rangle_t} = \frac{\langle a\rangle - \overline{d(t)}\langle b\rangle}{\sqrt{1+|d(t)|^2}},$$
$$\langle b^\dagger\rangle_t = \overline{\langle b\rangle_t} = \frac{\langle b^\dagger\rangle + \overline{d(t)}\langle a^\dagger\rangle}{\sqrt{1+|d(t)|^2}},$$
$$\langle a^\dagger a\rangle_t = \frac{\langle a^\dagger a\rangle + |d(t)|^2\langle b^\dagger b\rangle - \overline{d(t)}\langle a^\dagger b\rangle - d(t)\langle ab^\dagger\rangle}{1+|d(t)|^2},$$
$$\langle b^\dagger b\rangle_t = \frac{|d(t)|^2\langle a^\dagger a\rangle + \langle b^\dagger b\rangle + \overline{d(t)}\langle a^\dagger b\rangle + d(t)\langle ab^\dagger\rangle}{1+|d(t)|^2},$$
$$\langle ab^\dagger\rangle_t = \overline{\langle a^\dagger b\rangle_t} = \frac{\overline{d(t)}\langle a^\dagger a\rangle - \overline{d(t)}\langle b^\dagger b\rangle - \overline{d(t)}^2\langle a^\dagger b\rangle + \langle ab^\dagger\rangle}{1+|d(t)|^2}$$

and

$$\langle (a^\dagger a)^2\rangle_t = \frac{1}{(1+|d(t)|^2)^2}\left[\langle (a^\dagger a)^2\rangle + |d(t)|^4\langle (b^\dagger b)^2\rangle + 4|d(t)|^2\langle a^\dagger a b^\dagger b\rangle - 4\mathfrak{Re}[d(t)\langle a^\dagger a a b^\dagger\rangle]\right.$$
$$-4\mathfrak{Re}[d(t)|d(t)|^2\langle b^\dagger b a b^\dagger\rangle] + 2\mathfrak{Re}[d(t)^2\langle (ab^\dagger)^2\rangle] - 2(1-|d(t)|^2)\mathfrak{Re}[d(t)\langle ab^\dagger\rangle]$$
$$\left.+|d(t)|^2\langle b^\dagger b\rangle + |d(t)|^2\langle a^\dagger a\rangle\right],$$
$$\langle a^\dagger a b^\dagger b\rangle_t = \frac{1}{(1+|d(t)|^2)^2}\left[|d(t)|^2\langle (a^\dagger a)^2\rangle + |d(t)|^2\langle (b^\dagger b)^2\rangle + (1+|d(t)|^4 - 2|d(t)|^2)\langle a^\dagger a b^\dagger b\rangle\right.$$
$$+2(1-|d(t)|^2)\mathfrak{Re}[d(t)\langle a^\dagger a a b^\dagger\rangle] - 2(1-|d(t)|^2)\mathfrak{Re}[d(t)\langle b^\dagger b a b^\dagger\rangle]$$
$$\left.+2(1-|d(t)|^2)\mathfrak{Re}[d(t)\langle ab^\dagger\rangle] - 2\mathfrak{Re}[d(t)^2\langle (ab^\dagger)^2\rangle] - |d(t)|^2\langle b^\dagger b\rangle - |d(t)|^2\langle a^\dagger a\rangle\right].$$

The expectation values on the right sides of the above equations are the expectation values at $t=0$, i.e., we have written $\langle .\rangle(0)$ as $\langle .\rangle$, etc., for convenience. Some of these with respect to the state $|\psi(0)\rangle$ are listed as

$$\langle a^\dagger a\rangle = n_a,\ \ \langle (a^\dagger a)^2\rangle = n_a^2,$$
$$\langle b^\dagger b\rangle = n_b,\ \ \langle (b^\dagger b)^2\rangle = n_b^2,$$
$$\langle a^\dagger b\rangle = \overline{\langle ab^\dagger\rangle} = 0,\ \ \langle (a^\dagger b)^2\rangle = \overline{\langle (ab^\dagger)^2} = 0,$$
$$\langle a^\dagger a a b^\dagger\rangle = \overline{\langle a^\dagger b a^\dagger a\rangle} = 0,$$
$$\langle b^\dagger b a b^\dagger\rangle = \overline{\langle a^\dagger b a^\dagger a\rangle} = 0,$$
$$\langle a^\dagger a b^\dagger b\rangle = \overline{\langle (a^\dagger b)^2\rangle} = n_a n_b,$$

Funding Declaration

The authors declare that no funds, grants, or other support were received during the preparation of this manuscript.

References

[1] R. Loudon and P. L. Knight, 'Squeezed light,' J. Mod. Opt. 34, 709 (1987).

[2] D. F. Walls, 'Squeezed states of light,' Nature 306, 141 (1983).

[3] D. F. Walls, 'Evidence for the quantum nature of light,' Nature 280, 451 (1979).

[4] C. H. Bennett and S. J. Wiesner, 'Communication via one-and two-particle operators on Einstein-Podolsky-Rosen states,' Phys. Rev. Lett. 69, 2881 (1992).

[5] M. Hillery, 'Quantum cryptography with squeezed states,' Phys. Rev. A 61, 022309 (2000).

[6] A. Furusawa, J. L. Sorensen, S. L. Braunstein, C. A. Fuchs, H. J. Kimble, and E. S. Polzik, 'Unconditional quantum teleportation,' Science 282, 706 (1998).

[7] Z. Yuan, B. E. Kardynal, R. M. Stevenson, A. J. Shields, C. J. Lobo, K. Cooper, N. S. Beattie, D. A. Ritchie, and M. Pepper, 'Electrically driven single-photon source,' Science 295, 102 (2002).

[8] U. L. Andersen, G. Leuchs, and C. Silberhorn, 'Continuous-variable quantum information processing,' Laser and Photonics Rev. 4, 337 (2010).

[9] H. K. Lau and M. B. Plenio, 'Universal quantum computing with arbitrary continuous-variable encoding,' Phys. Rev. Lett. 117, 100501 (2016).

[10] A. S. Parkins and H. J. Kimble, 'Quantum state transfer between motion and light,' J. Opt. B: Quantum Semiclass. Opt. 1, 496 (1999).

[11] V. Falch, A. Brataas, and A. Qaiumzadeh, 'Second-order correlation and squeezing of photons in cavities with ultrastrong magnon-photon interactions' Phys. Rev. B 111, 104425 (2025)

[12] W. H. Louisell, A. Yariv, and A. E. Siegman, 'Quantum fluctuations and noise in parametric processes. I.,' Phys. Rev. 124, 1646 (1961).

[13] L. Tian and Z. Li, 'Quantum frequency conversion and quantum networks,' npj Quantum Info. 6, 89 (2020).

[14] N. Sangouard, C. Simon, H. de Riedmatten, and N. Gisin, 'Quantum repeaters based on atomic ensembles and linear optics,' Rev. Mod. Phys. 83, 33 (2011).

[15] Y. C. Lu. Eugene, 'Quantum Theory of Nonlinear Optical Processes with Time-Dependent Pump Amplitude and Phase: Frequency Conversion,' Phys. Rev. A 8, 1053 (1973).

[16] Y. Zuo, R. Huang, L.-M. Kuang, X.-W. Xu, and H. Jing, 'Loss-induced suppression, revival, and switch of photon blockade,' Phys. Rev. A 106, 043715 (2022).

[17] R. Usefi and M. K. Tavassoly, 'The effect of quantum frequency conversion on the quantumness of radiation field states,' Optik 321, 172172 (2025).

[18] J. J. Sakurai and J. Napolitano, *Modern Quantum Mechanics*, 3rd ed. (Cambridge University Press, 2020).

[19] H. R. Lewis, Jr., Phys. Rev. Lett. 18, 510 (1967).

[20] H. R. Lewis, Jr., and W. B. Riesenfeld, J. Math. Phys. 10, 1458 (1969).

[21] C. M. Caves, 'Quantum limits on noise in linear amplifiers,' Phys. Rev. D 26, 1817 (1982).

[22] L. Mandel and E. Wolf, *Optical Coherence and Quantum Optics* (Cambridge University Press, 1995).

[23] R. Takagi and Q. Zhuang, 'Convex resource theory of non-Gaussianity,' Phys. Rev. A 97, 062337 (2018).

[24] N. Khaneja, T. Reiss, C. Kehlet, T. Schulte-Herbrggen, and S. J. Glaser, 'Optimal control of coupled spin dynamics: design of NMR pulse sequences by gradient ascent algorithms,' J. Magn. Reson. 172, 296 (2005).

[25] T. Caneva, T. Calarco, and S. Montangero, 'Chopped random-basis quantum optimization,' Phys. Rev. A 84, 022326 (2011).

[26] G. Adesso and F. Illuminati, 'Entanglement in continuous-variable systems: recent advances and current perspectives,' J. Phys. A: Math. Theor. 40, 7821 (2007).

[27] Z. L. Xiang, S. Ashhab, J. Q. You, and F. Nori, 'Hybrid quantum circuits: Superconducting circuits interacting with other quantum systems,' Rev. Mod. Phys. 85, 623 (2013).

[28] T. Yu and J. H. Eberly, 'Finite-time disentanglement via spontaneous emission,' Phys. Rev. Lett. 93, 140404 (2004).

[29] G. Giedke and J. I. Cirac, 'Characterization of Gaussian operations and distillation of Gaussian states,' Phys. Rev. A 66, 032316 (2002).

[30] A. Joseph, M. A. Smith, M. P. Weides, and R. Macedo, 'Dynamic Modulation of Long-Range Photon-Magnon Coupling,' arXiv:2512.02732 [quant-ph] (2025).

[31] M. Asano, H. Okamoto, and H. Yamaguchi, 'Synthesized Kuramoto potential via optomechanical Floquet engineering,' Sci. Adv. 11, eady4167 (2025).

[32] D. F. Walls and R. Barakat, Phys. Rev. A 1, 446 (1970).

[33] J. Tucker and D. F. Walls, Phys. Rev. 178, 2036 (1969).

[34] M. Rodrigo, 'The time dependent susceptibility of spin glasses,' Phys. Lett. A 70, 227 (1979).

[35] H. Kliem and B. Schumacher, 'Time-dependent dielectric susceptibility in high electric fields,' IEEE Trans. Electr. Insul. EI-22, 219 (1987).

[36] G. Gnter, A. A. Anappara, J. Hees, A. Sell, G. Biasiol, L. Sorba, S. De Liberato, C. Ciuti, A. Tredicucci, A. Leitenstorfer, and R. Huber, 'Sub-cycle switch-on of ultrastrong light-matter interaction,' Nature 458, 178 (2009).

[37] R. Chamakhi, A. Gauthier, T. Bourdel, and M. Giraud, 'Fast momentum-selective transport of Bose-Einstein condensates via controlled non-adiabatic dynamics in optical lattices,' arXiv:2509.16367 [cond-mat.quant-gas] (2025).

[38] C. N. Barrett, S. Majumder, R. Sensarma, and V. Tripathi, 'Nonadiabatic Parametric Control Through the Lens of Landau-Zener Interference and Resonant Driving,' APS Global Physics Summit (2025).

[39] K. Pang, A. A. Basharin, V. A. Fedotov, and A. V. Zayats, 'Adiabatic Frequency Conversion Using a Time-Varying Epsilon-Near-Zero Metasurface,' Nano Lett. 21, 5907 (2021).

[40] G. Watanabe and H. Makela, Phys. Rev. A 85, 053624 (2012).

[41] R.-X. Chen, L.-T. Shen, Z.-B. Yang, and H.-Z. Wu, Phys. Rev. A 91, 012312 (2015).

[42] H. Ollivier and W. H. Zurek, 'Quantum Discord: A Measure of the Quantumness of Correlations,' Phys. Rev. Lett. 88, 017901 (2001).

[43] W. H. Zurek, 'Decoherence, einselection, and the quantum origins of the classical,' Rev. Mod. Phys. 75, 715 (2003).

[44] D. F. Walls and G. J. Milburn, *Quantum Optics*, 2nd ed. (Springer-Verlag, 2008).

[45] C. K. Hong, Z. Y. Ou, and L. Mandel, 'Measurement of subpicosecond time intervals between two photons by interference,' Phys. Rev. Lett. 59, 2044 (1987).

[46] C. Hamsen, K. N. Tolazzi, T. Wilk, and G. Rempe, 'Two-photon blockade in an atom-driven cavity QED system,' Phys. Rev. Lett. 118, 133604 (2017).

[47] L. A. Lugiato and G. Strini, 'On nonclassical effects in two-photon optical bistability and two-photon laser,' Opt. Commun. 41, 67 (1982).

[48] A. Miranowicz, J. Bajer, M. Paprzycka, Y.-X. Liu, A. M. Zagoskin, and F. Nori, 'Theoretical study of two-photon blockade in Kerr nonlinear cavities,' Phys. Rev. A 87, 023809 (2013).

[49] H. J. Carmichael, 'Analyzed photon blockade in driven nonlinear cavities,' Phys. Rev. X 5, 031028 (2015).

[50] A. Faraon, I. Fushman, D. Englund, N. Stoltz, P. Petroff, and J. Vuckovic, 'Experimental demonstration of photon blockade in photonic crystal cavities,' Nat. Phys. 4, 859 (2008).

[51] Q.-C. Wu, T. Liu, Y.-H. Zhou, and C.-P. Yang, 'Two-photon blockade with second-order nonlinearity in cavity systems,' Int. J. Theor. Phys. 61, 21 (2022).

[52] H.-P. Breuer and F. Petruccione, *The Theory of Open Quantum Systems* (Oxford University Press, 2002).

[53] S. Diehl, A. Micheli, A. Kantian, B. Kraus, H. P. Bchler, and P. Zoller, 'Quantum states and phases in driven open quantum systems with cold atoms,' Nat. Phys. 4, 878 (2008).

[54] P. Komr, E. M. Kessler, M. Bishof, L. Jiang, A. S. Srensen, J. Ye, and M. D. Lukin, 'A quantum network of clocks,' Nat. Phys. 10, 582 (2014).

[55] R. Kumar, A. Das, S. Ghosh, and A. K. Das, 'Quantum frequency conversion for quantum networks,' Opt. Express 30, 23154 (2022).

[56] J. Hu, H. Yuan, J. Akin, A. K. M. Naziul Haque, Y. Zhao, and K. Fang, 'Efficient bidirectional quantum frequency conversion between telecom and visible bands using programmable III-V nanophotonic waveguides,' arXiv:2510.16696 [quant-ph] (2025).

[57] P. O. Weigel, M. Savanier, C. T. DeRose, A. T. Pomerene, A. L. Starbuck, A. L. Lentine, V. Stenger, and S. Mookherjea, 'Lightwave circuits in lithium niobate through hybrid waveguides with silicon photonics,' Sci. Adv. 2, e1600256 (2016).

[58] N. Matsuda, R. Shimizu, Y. Mitsumori, H. Kosaka, and K. Edamatsu, 'All-optical phase modulations in a silicon-wire waveguide,' Nat. Photonics 10, 366 (2016).

[59] M. A. Castellanos-Beltran, K. D. Irwin, G. C. Hilton, L. R. Vale, and K. W. Lehnert, 'Amplification and squeezing of quantum noise with a tunable Josephson metamaterial,' Nat. Phys. 4, 929 (2008).

[60] E. Flurin, N. Roch, F. Mallet, M. Devoret, and B. Huard, 'Generating Entangled Microwave Radiation Over Two Transmission Lines,' Phys. Rev. Lett. 109, 183901 (2012).

[61] M. Aspelmeyer, T. J. Kippenberg, and F. Marquardt, 'Cavity optomechanics,' Rev. Mod. Phys. 86, 1391 (2014).

[62] A. Alocco, L. Planat, and N. Roch, 'Programmable Microwave Cluster States via Josephson Metamaterials,' in preparation (2025).

[63] Y.-D. Wang, F. Zou, and A. A. Clerk, 'Reconfiguration of Quantum Photonic Integrated Circuits Using Auxiliary Fields,' Laser Photonics Rev. 19, 2401023 (2025).

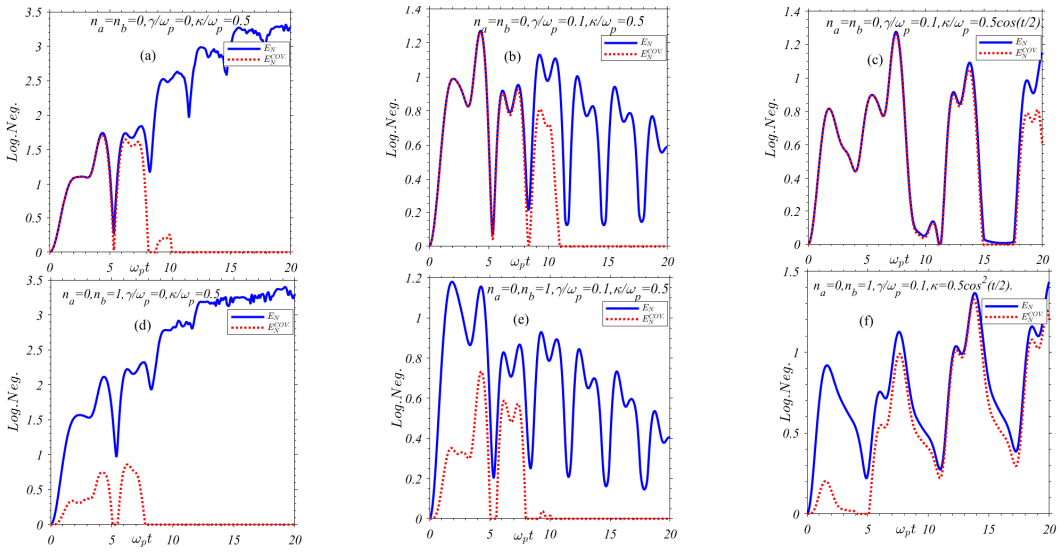


Figure 1: The Logarithmic Negativity E_N (solid Blue), and $E_N^{COV.}$ (dotted green) **for** the states $U_{QFC}(t)|0,0\rangle$ (a,b,c), and $U_{QFC}(t)|0,1\rangle$ (d,e,f) attached to a system of the Hamiltonian $H(t) = \hbar\omega_a a^\dagger a + \hbar\omega_b b^\dagger b - \hbar\kappa\cos(\omega_p t + \theta)(a^\dagger - a)(b^\dagger - b)$, as function of a scaled time $\omega_p t$ for a constant as well as different time-dependent coupling coefficients $\kappa/\omega_p = 0.5$ (a,b,d,e), $\kappa/\omega_p = 0.5\cos(t/2)$ (c), and $\kappa/\omega_p = 0.5\cos^2(t/2)$ (f) with different decay rates $\gamma/\omega_p = 0$ (a,d) and $\gamma/\omega_p = 0.1$ (b,c,e,f) with $\omega_a = \omega_b = \omega_p = 1$, $\theta = \pi/2$.

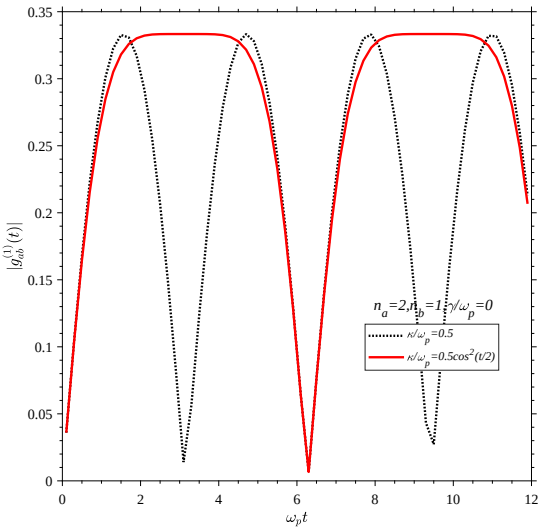


Figure 2: The coherence function $g_{ab}^{(1)}(t)$ **for** an output state $U_{QFC}(t)|2,1\rangle$, attached to a system of the quantum frequency converter, as function of a scaled time $\omega_p t$ for different coupling coefficients: $\kappa/\omega_p = 0.5$ (Dotted), and $\kappa/\omega_p = 0.5\cos^2(\frac{t}{2})$ (Solid).

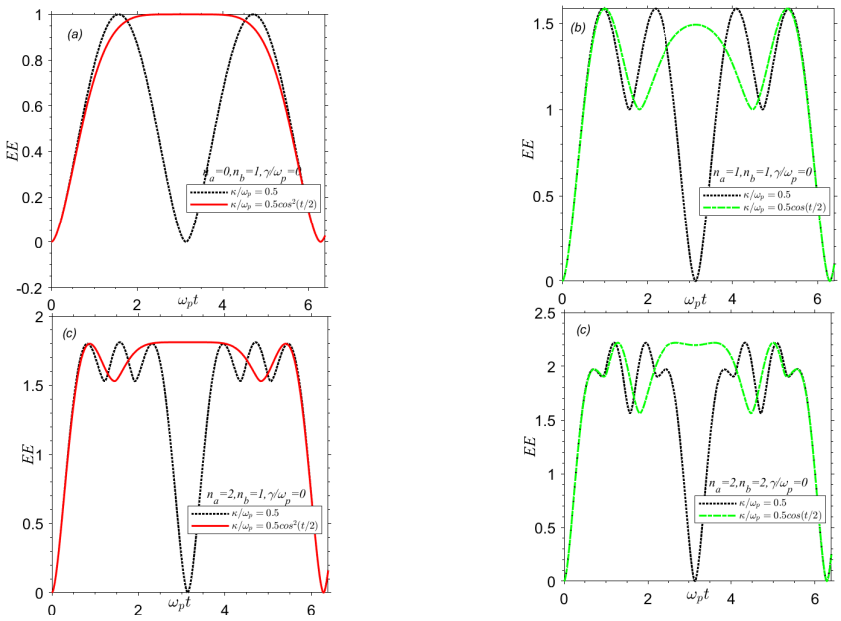


Figure 3: The entanglement entropy $S_a(t)$ **for** the states $U_{QFC}(t)|0,1\rangle$ (a), $U_{QFC}(t)|2,1\rangle$ (b), and $U_{QFC}(t)|1,1\rangle$ (c), $U_{QFC}(t)|2,2\rangle$ (d) attached to a system of the quantum frequency converter, as function of a scaled time $\omega_p t$ for different coupling coefficients: $\kappa/\omega_p = 0.5$ (Dotted, Black), $\kappa/\omega_p = \frac{1}{2}\cos(\frac{t}{5})$ (Solid, Red), and $\kappa/\omega_p = \frac{1}{2}\cos^2(\frac{t}{2})$ (Dot-Dashed, Green).$\omega_a = 2, \omega_b = \omega_p = 1$

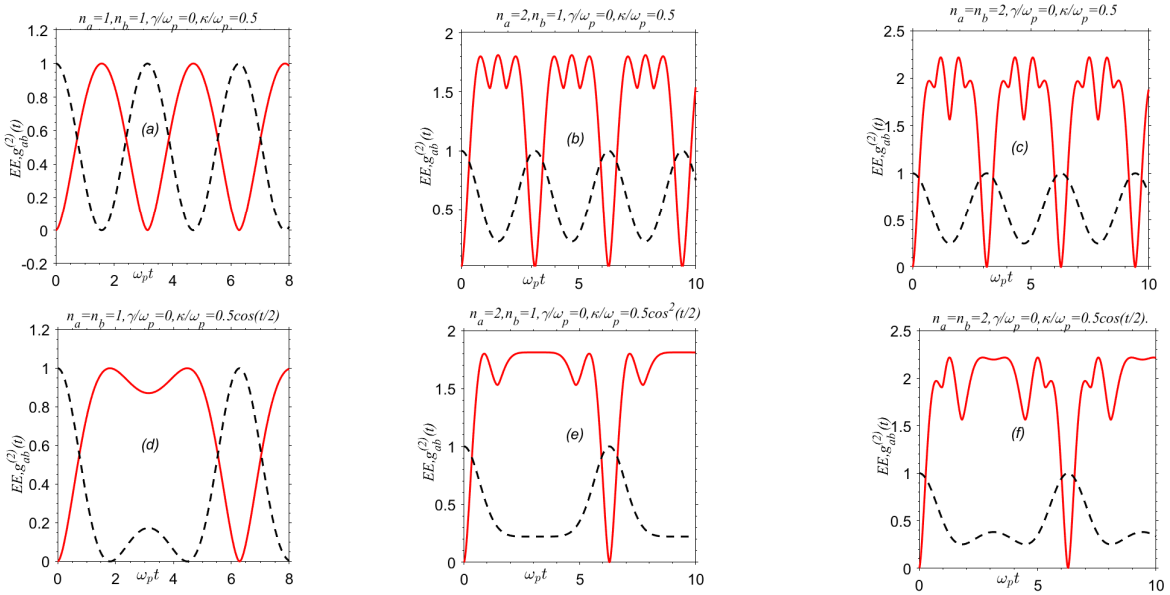


Figure 4: The entanglement entropy $S_a(t)$ for the states $U_{QFC}(t)|1,1\rangle$ (a,d), $U_{QFC}(t)|2,1\rangle$ (b,e), and $U_{QFC}(t)|2,2\rangle$ (c,f) attached to a system of the quantum frequency converter, as function of a scaled time $\omega_p t$ for different coupling coefficients: $\kappa/\omega_p = 0.5$ (a,b,c), $\kappa/\omega_p = 0.5\cos(\frac{t}{2})$ (d,f), and $\kappa/\omega_p = 0.5\cos^2(\frac{t}{2})$ (e).

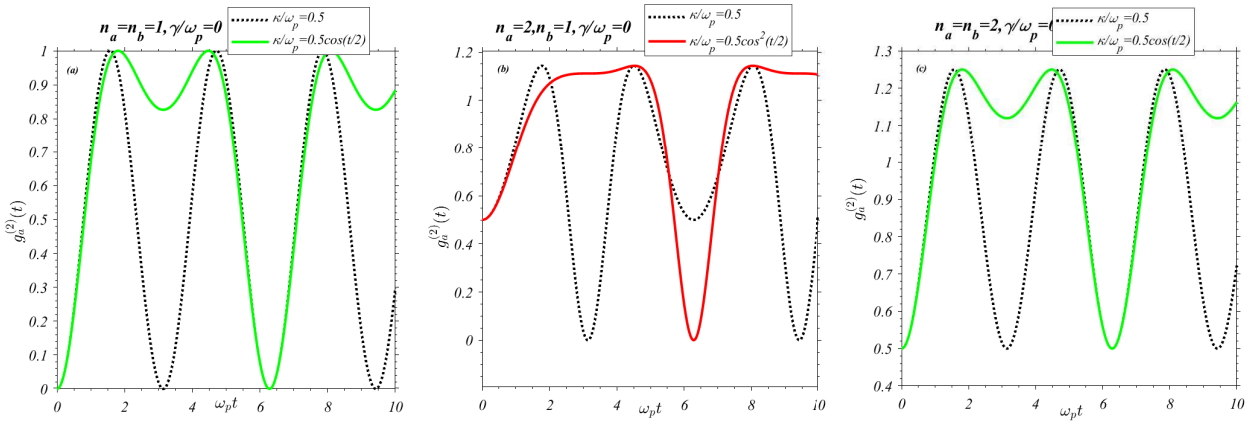


Figure 5: Study of the bunching process by the second order correlation function $g_a^{(2)}(t)$ for the states $U_{QFC}(t)|1,1\rangle$ (a), $U_{QFC}(t)|2,1\rangle$ (b), and $U_{QFC}(t)|2,2\rangle$ (c) attached to a system of the quantum frequency converter, as function of a scaled time $\omega_p t$ for different coupling coefficient, $\kappa/\omega_p = 0.5$ (Dotted), $\kappa/\omega_p = 0.5\cos(\frac{t}{2})$ (Green-Solid), and $\kappa/\omega_p = 0.5\cos^2(\frac{t}{2})$ (Red-Solid).

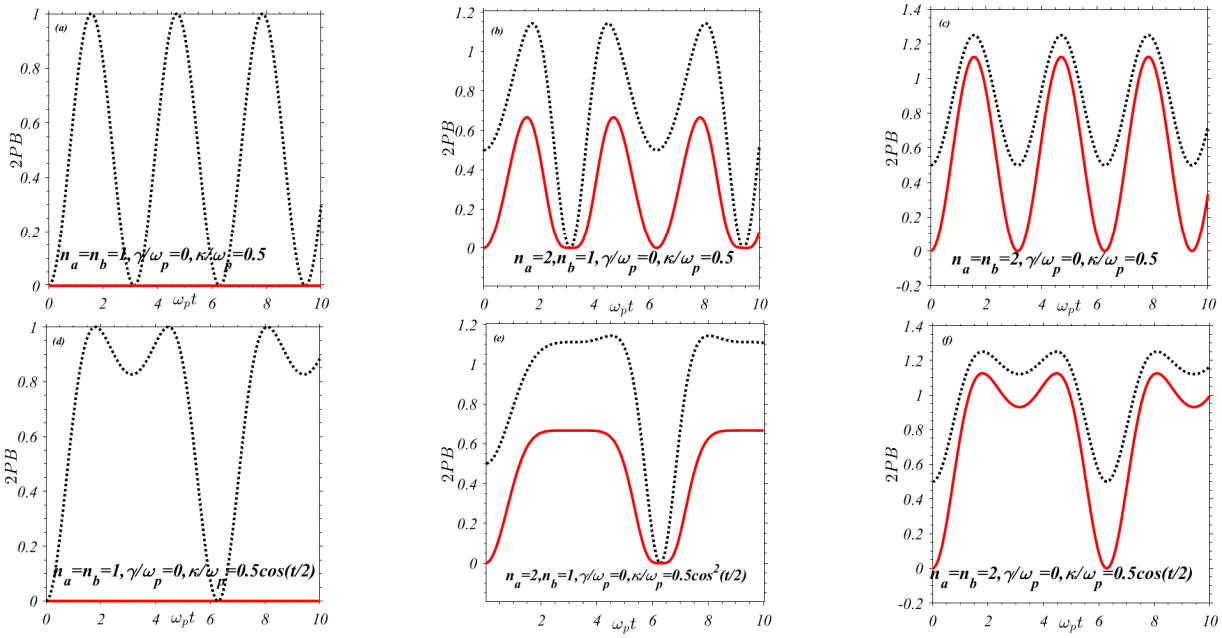


Figure 6: Study of the two-photon blockade process by simultaneously considering both the equal-time second order and third order correlation functions $g_a^{(2)}(t)$ (Dotted line) and $g_a^{(3)}(t)$ (Solid line) as functions of a scaled time $\omega_p t$ with different coupling coefficients $\kappa/\omega_p = 0.5$ (Top row), $\kappa/\omega_p = 0.5\cos(t/2)$ (d,f), and $\kappa/\omega_p = 0.5\cos^2(t/2)$ (e). This is attached to the quantum frequency converter where the system is initially prepared in tensor-product states as $U_{\text{fc.}}(t)|0,1\rangle$ (a,d), $U_{\text{fc.}}(t)|1,1\rangle$ (b,e), and $U_{\text{fc.}}(t)|2,1\rangle$ (c,f).

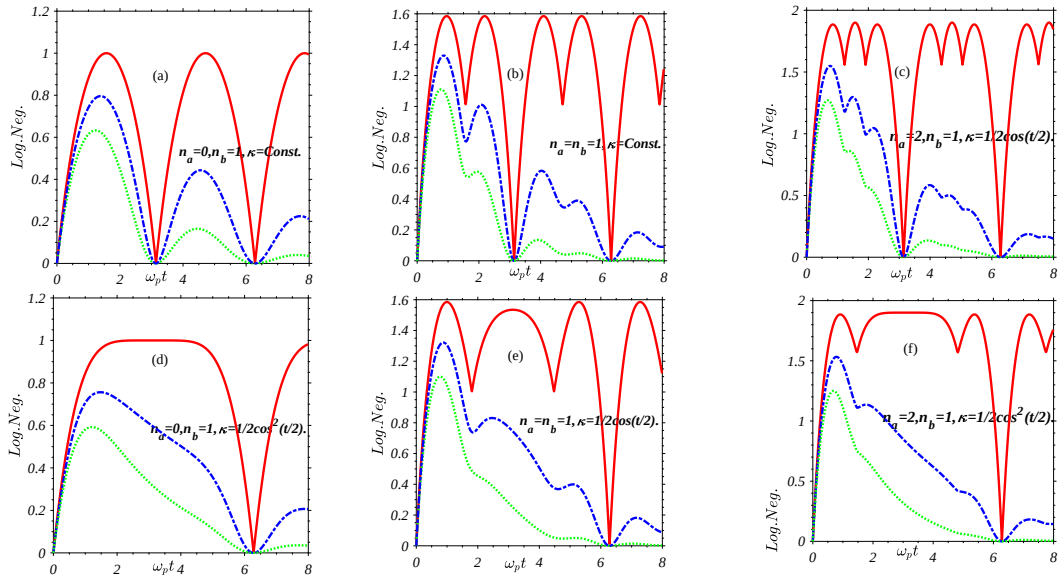


Figure 7: Temporal evolution of quantum entanglement via logarithmic negativity E_N for the quantum frequency converter. Initial states are: (a,d) $U_{QFC}(t)|0,1\rangle$, (b,e) $U_{QFC}(t)|1,1\rangle$, and (c,f) $U_{QFC}(t)|2,1\rangle$. Coupling configurations: constant $\kappa/\omega_p = 0.5$ (a-c); time-dependent $\kappa/\omega_p = 0.5\cos(t/2)$ (d,f) and $\kappa/\omega_p = 0.5\cos^2(t/2)$ (e). Line styles correspond to decay rates: $\gamma/\omega_p = 0$ (solid red), $\gamma/\omega_p = 0.1$ (dash-dotted blue), and $\gamma/\omega_p = 0.2$ (dotted green).